Mon. Not. R. Astron. Soc. **376,** 793–808 (2007) doi:10.1111/j.1365-2966.2007.11474.x

Statistical equilibrium and ion cyclotron absorption/emission in strongly magnetized plasmas

Alexander Y. Potekhin[1,2]★ and Dong Lai[2]

[1] *Ioffe Physico-Technical Institute, Politekhnicheskaya 26, 194021 St. Petersburg, Russia*
[2] *Center for Radiophysics and Space Research, Department of Astronomy, Cornell University, Ithaca, NY 14853, USA*

Accepted 2007 January 5. Received 2006 November 30

ABSTRACT

We calculate the transition rates between proton Landau levels due to non-radiative and radiative Coulomb collisions in an electron–proton plasma with strong magnetic field B. Both electron–proton collisions and proton–proton collisions are considered. The roles of the first-order cyclotron absorption and second-order free–free absorption and scattering in determining the line strength and shape as well as the continuum are analysed in detail. We solve the statistical balance equation for the populations of proton Landau levels. For temperatures $\sim 10^6$–10^7 K, the deviations of the proton populations from local thermal equilibrium are appreciable at density $\rho \lesssim 0.1\, B_{14}^{3.5}\ \mathrm{g\,cm^{-3}}$, where $B_{14} = B/(10^{14}\ \mathrm{G})$. We present general formulae for the plasma emissivity and absorption coefficents under a wide range of physical conditions. Our results are useful for studying the possibility and the conditions of proton/ion cyclotron line formation in the near vicinity of highly magnetized neutron stars.

Key words: magnetic fields – plasmas – stars: neutron – X-rays: stars.

1 INTRODUCTION

Cyclotron lines are a powerful diagnostic tool for magnetized neutron stars. The detection of electron cyclotron features at 10–80 keV in the spectra of a number of binary X-ray pulsars (e.g. Trümper et al. 1978; see Heindl et al. 2004; Terada et al. 2006 for recent observations) provided direct confirmation that these are neutron stars endowed with strong magnetic fields $B \sim 10^{12}$–10^{13} G. Numerous theoretical works have been devoted to the physics and modelling of electron cyclotron line formation and transfer in accreting neutron stars (e.g. Wasserman & Salpeter 1980; Mészáros & Nagel 1985; Burnard, Klein & Arons 1988; Lamb, Wang & Wasserman 1990; Wang, Wasserman & Lamb 1993; Araya & Harding 1999; Araya-Góchez & Harding 2000).

There has been growing evidence in recent years for the existence of neutron stars possessing superstrong magnetic fields, $B \gtrsim 10^{14}$ G. In particular, soft gamma-ray repeaters (SGRs) and anomalous X-ray pulsars (AXPs) are believed to be magnetars, whose radiation is powered by the decay of superstrong magnetic fields (see Thompson & Duncan 1995, 1996; Woods & Thompson 2005). Several radio pulsars with inferred surface magnetic fields approaching 10^{14} G have also been discovered (e.g. McLaughlin et al. 2003). In such superstrong magnetic field regime, the electron cyclotron energy,

$$\hbar\omega_{\rm ce} = \hbar\,\frac{eB}{m_{\rm e}c} = 1.16\ B_{14}\,\mathrm{MeV}, \qquad (1)$$

lies outside the X-ray band, but the ion cyclotron energy,

$$\hbar\omega_{\rm ci} = \hbar\,\frac{ZeB}{m_{\rm i}c} = 0.635\,(Z/A)B_{14}\,\mathrm{keV}, \qquad (2)$$

lies in the detectable range for X-ray telescopes such as *Chandra* and *XMM–Newton* when $B_{14} \gtrsim 0.4$. In equations (1) and (2), $B_{14} = B/(10^{14}\ \mathrm{G})$, $m_{\rm i}$ is an ion mass and Z and A are nuclear charge and mass numbers. In the last few years, absorption features at $E \sim 0.2$–1 keV have been detected in the spectra of several thermally emitting isolated neutron stars (e.g. Haberl et al. 2004; van Kerkwijk et al. 2004; van Kerkwijk & Kaplan 2006). While no definitive identifications of the lines have been made, it is likely that some of these lines involve proton cyclotron resonances at $B \lesssim 10^{14}$ G. Somewhat surprisingly, the observed quiescent emission of AXPs and SGRs does not show any spectral feature, in particular the proton cyclotron line around 1 keV (e.g. Juett et al. 2002; Kulkarni et al. 2003; Patel et al. 2003; Tiengo et al. 2005). This absence of lines may be naturally explained by the effect of vacuum polarization, which tends to reduce the line width significantly in the atmosphere (thermal) emission for $B \gtrsim 10^{14}$ G (Ho & Lai 2003, 2004; Lai & Ho 2003; van Adelsberg & Lai 2006).

There has been some evidence for ion cyclotron lines during several AXP/SGR outbursts, e.g. the 6.4-keV emission feature in SGR 1900+14 (Strohmayer & Ibrahim 2000), the 5-keV absorption feature in SGR 1806−20 (Ibrahim, Swank & Parke 2003) and the 14-keV emission feature (and possibly also ∼7, 30 keV features) in the bursts of AXP 1E 1048−5937 (Gavriil, Kaspi & Woods 2002). There was also a possible detection of a 8.1-keV absorption feature in AXP 1RXS J1708−4009 (Rea et al. 2003; but see Rea et al. 2005). It is possible that these absorption/emission features are produced

★E-mail: palex@astro.ioffe.ru

by ion cyclotron resonances in the corona or lower magnetosphere of magnetars (although one cannot exclude the alternative possibility that they are produced by electron cyclotron resonances in upper magnetospheres).

To be specific, in the following we focus on the electron–proton plasma ($Z = 1, A = 1.008$, spin $=1/2$) and the proton cyclotron resonance with energy $\hbar\omega_{\rm cp} = 0.630\,B_{14}$ keV. Generalization to other ions is outlined in Section 7.

While the physics of electron cyclotron line transfer has been extensively studied in the context of accreting X-ray pulsars (see above), several basic issues regarding proton cyclotron line have not been properly considered. Since the radiative electron cyclotron decay rate is many orders of magnitude larger than the collisional de-excitation rate, electron cyclotron resonance always takes the form of scattering (e.g. Mészáros 1992). For protons, the radiative cyclotron decay rate is much smaller, so the situation is not at all clear. Depending on the plasma density, temperature and magnetic field strength, true proton cyclotron absorption and emission are possible. Previous calculations of proton cyclotron lines from magnetized neutron star atmospheres (e.g. Zane et al. 2001; Ho & Lai 2001, 2003; Potekhin et al. 2004) assumed local thermal equilibrium (LTE) population of proton Landau levels. We will see that this assumption is not always valid in the case of a magnetar.

In this paper we study systematically the rates for collision-induced proton cyclotron transitions in a magnetized plasma. Combining these rates with radiative transition rates, we then study the statistical equilibrium of protons in different Landau levels, and use the non-LTE level population to calculate the radiative opacities and emissivities for different photon modes. Our results serve as an crucial ingredient for determining the possibility and the physical conditions of proton/ion cyclotron line formation in various plasma environments of highly magnetized neutron stars.

In statistical equilibrium, populations of excited Landau levels of the ions are determined by rates of spontaneous radiative decay and by rates of transitions caused by radiative and non-radiative Coulomb collisions (note that 'true' cyclotron absorption can be separated from scattering by considering second-order Feynman diagrams which include Coulomb interaction; cf. Daugherty & Ventura 1978). Order-of-magnitude estimates of the rates of these processes and their consequences for the level populations are given in Section 2. In subsequent sections we consider these processes in more detail. In Section 3 we write formulae for rates of such transitions in a proton–electron plasma. Radiative transition rates and cross-sections are considered in Section 4. In Section 5 we analyse population of the Landau states of the ions. Opacity and emissivity for the ion cyclotron resonance are calculated in Section 6.

1.1 Landau level basics and notations

Motion of the ions and electrons in the plane (xy) perpendicular to the magnetic field $\boldsymbol{B}$ (assumed to be directed along z) is quantized in Landau levels with excitation energies $E_{N,\perp} = mc^2\,[\sqrt{1+2bN} - 1]$ $(N = 0, 1, \ldots)$, where $b = \hbar\omega_{\rm c}/mc^2$ is the relativistic magnetic parameter, $\omega_{\rm c} = |Ze|B/mc$ is the cyclotron frequency, and Ze and m are the charge and mass of the particle (e is the elementary charge). For non-interacting particles, every Landau level is degenerate with respect to a position of the guiding centre in the xy plane (e.g. Landau & Lifshitz 1976). The number of degenerate states (for fixed N and longitudinal velocity v_z) is $L_x L_y\,|Z|/(2\pi a_{\rm m}^2)$, where

$$a_{\rm m} = \left(\frac{\hbar c}{eB}\right)^{1/2} = 2.5656 \times 10^{-11}\,B_{14}^{-1/2}\,{\rm cm} \qquad (3)$$

is the magnetic length, and L_x and L_y are normalization lengths. In addition, excited Landau levels of the electrons usually can be treated as double spin-degenerate. In contrast, the Landau levels of the ions are not degenerate, but split with respect to the spin, because of the anomalous magnetic moments of nuclei.

For the electrons, the relativistic magnetic parameter is $b_{\rm e} = \hbar\omega_{\rm ce}/(m_{\rm e}c^2) = B/B_{\rm Q}$, where $B_{\rm Q} = m_{\rm e}^2c^3/(e\hbar) = 4.414 \times 10^{13}$ G. For density $\rho \ll 7 \times 10^6 (A/Z) B_{14}^{3/2}\,{\rm g\,cm^{-3}}$ and temperature $T \ll \hbar\omega_{\rm ce}/k_B = 1.34 \times 10^{10} B_{14}$ K, virtually all electrons reside in the ground Landau level. For $T \gtrsim 2.7 \times 10^{-4}\,B_{14}^{-2}\,(\rho_0 Z/A)^2$ K (where ρ_0 is the density in units of 1 g cm^{-3}), the electrons are non-degenerate. We shall be concerned with this regime in this paper.

For the ions, the cyclotron energy is $\hbar\omega_{\rm ci} = 0.635\,(Z/A)\,B_{14}$ keV, and their relativistic magnetic parameter is $b_{\rm i} = \hbar\omega_{\rm ci}/(m_{\rm i}c^2) = b_{\rm e}Z(m_{\rm e}/m_{\rm i})^2 = 0.68 \times 10^{-6}(Z/A^2)\,B_{14}$. We consider the situation where the ions are non-relativistic: $Nb_{\rm i} \ll 1$, $E_{N,\perp} = N\hbar\omega_{\rm ci}$. Obviously it is always the case if the ion Landau number N is not huge.

In the following we introduce a number of notations for various kinds of transition rates (i.e. number of transitions per unit time per occupied initial state) between proton Landau levels N and N' and corresponding cross-sections. Here we list these and other related notations and the basic relevant equations for easy reference:

$\omega_{\rm ce}$, $\omega_{\rm ci}$, $\omega_{\rm cp}$	cyclotron frequencies for electron, ion and proton: equations (1), (2)
$a_{\rm m}$	magnetic length: equation (3)
$n_{\rm e}$, $n_{\rm i}$, $n_{\rm p}$	number densities of electrons, ions and protons in the plasma
n_N	number density of protons in the Nth Landau level ($N = 0, 1, 2, $)
$W^{\rm fix}_{NN'}(v_z)$	transition rate per particle on the level N with initial longitudinal (i.e. along $\boldsymbol{B}$) velocity v_z, in a volume V for scattering on a fixed Coulomb centre: equation (A7)
$\sigma^{\rm fix}_{NN'}(v_z)$	corresponding cross-section: equations (A7) and (A13)
$W^{\rm (pe)}_{NN'}(v_z)$	transition rate for protons scattered on those electrons which rest on the ground Landau level, assuming the relative initial longitudinal velocity v_z: equation (8)
$\sigma^{\rm (pe)}_{NN'}(v_z)$	partial cross-section for such scattering, normalized to v_z: equations (4) and (8)
$W_{N_1N_2;N_1'N_2'}(v_z)$	transition rate for charged particle 1 scattered on particle 2 in volume V at relative longitudinal velocity v_z, under the condition that initial and final Landau numbers of particle i are N_i and N_i', respectively: equation (A19)

$W^{\pm}_{N_1,N_2;N_1',N_2'}(v_z)$	analogous to $W_{N_1N_2;N_1'N_2'}(v_z)$, but for collision of identical particles with even (+) or odd (−) total spin: equation (A22)
$\sigma^{(\mathrm{pp})\pm}_{NN_2;N'N_2'}$	corresponding cross-section normalized to v_z: equations (15), (16) and (A19)
$\sigma^{(N_2)}_{NN'}$	partial cross-section of a proton with initial Landau number N_2 (regardless of its final Landau number) with respect to scattering of a test proton from Landau number N to N': equation (18)
$\Gamma^{C(\mathrm{pe})}_{NN'}$	velocity-averaged partial Coulomb transition rate for proton scattering on the electrons on the ground Landau level: equations (4), (7) and (12)
$\Gamma^{C(\mathrm{pp})}_{NN'}$	analogous to $\Gamma^{C(\mathrm{pe})}_{NN'}$, but because of collisions with other protons: equations (15) and (18)
$\Gamma^{A}_{NN'}$	spontaneous decay rate: equations (5), (21) and (28)
$\Gamma^{B}_{NN'}$	total transition rate due to photoabsorption: equations (20) and (30)
$\hat{\Gamma}^{B}_{NN'}$	total transition rate due to stimulated emission: equation (30)
$\sigma_{NN'}(j,\omega,\mathbf{n})$	cross-section of a proton with respect to photoabsorption (normalized to speed of light) for polarization j ($j = 1, 2$), photon frequency ω and direction $\mathbf{n}$: equations (24), (25), (26) and (47)
$\sigma_{\alpha,NN'}(\omega)$	partial photoabsorption cross-section (normalized to speed of light) for basic polarization α ($\alpha = 0, \pm 1$): equations (25), (26) and (28)
$\sigma^{\mathrm{ff}}_{\alpha}(\omega)$, $\sigma^{\mathrm{ff}}_{\alpha,NN'}(\omega)$	total and partial cross-sections (normalized to speed of light) for basic polarization α, for transitions caused by free–free photoabsorption of a proton–electron pair: equations (33), (34) and (B1)
$\sigma_{NN'}(v_z,\omega)$	partial cross-section $\sigma_{\alpha,NN'}(\omega)$ for longitudinal velocity v_z of the absorbing particle: equations (46) and (50)
$\sigma^{\mathrm{sc}}_{\alpha}$	cross-section of a proton with respect to scattering of a photon for basic polarization α: equation (37).

2 ORDER-OF-MAGNITUDE ESTIMATE FOR PROTON LANDAU LEVEL POPULATIONS

In this section we present simple estimates of the relative population of protons in the ground Landau level (number density n_0) and the first excited level (n_1). Other levels are neglected here for simplicity, and also for simplicity we assume that transitions stimulated by radiation are unimportant. The cyclotron energy of the proton is $\hbar\omega_{\mathrm{cp}} = \hbar(eB/m_{\mathrm{p}}\,c) \approx 0.63\,B_{14}$ keV. In this section we use without proof formulae for the rates of transitions between proton Landau levels, deferring their derivation to the following sections.

(i) **Coulomb collisions.** The collisional cross-section involving proton Landau transition $N = 1 \to N = 0$ is denoted by $\sigma^{(\mathrm{pe})}_{10}(v_z)$, where v_z is the relative velocity (along the z-axis) between the electron and the ion before collision. Detailed balance implies $\sigma^{(\mathrm{pe})}_{10}(v_z) = \sigma^{(\mathrm{pe})}_{01}(v_z')$, where v_z and v_z' are related by $m_* v_z^2/2 + \hbar\omega_{\mathrm{cp}} = m_* v_z'^2/2$, and $m_* = m_{\mathrm{e}} m_{\mathrm{i}}/(m_{\mathrm{e}} + m_{\mathrm{i}}) \simeq m_{\mathrm{e}}$ is the reduced mass. The collisional deexcitation rate per proton is

$$\Gamma^{C(\mathrm{pe})}_{10} = n_{\mathrm{e}}\langle v_z \sigma_{10}(v_z)\rangle = 4\sqrt{2\pi}\,n_{\mathrm{e}}\,\frac{a_{\mathrm{m}}^3 e^4\sqrt{m_{\mathrm{p}} m_*}}{\hbar^3}\,\tilde{\Lambda}^{(\mathrm{pe})}_{10}, \tag{4}$$

where n_{e} is the electron number density, $\langle\ldots\rangle$ denotes averaging over the 1D Maxwell distribution $f(v) \propto \exp(-m_* v^2/2T)$, and the Coulomb logarithm $\tilde{\Lambda}^{(\mathrm{pe})}_{10}$ (to be defined later) is of order of unity for the plasma parameters we are interested in. In general, $\tilde{\Lambda}^{(\mathrm{pe})}_{10}$ depends on parameter $\beta_{\mathrm{p}} \equiv \hbar\omega_{\mathrm{cp}}/T = 73.38\,B_{14}/T_6$, where T is the kinetic temperature for particle motion along $\boldsymbol{B}$, and $T_6 \equiv T/(10^6\,\mathrm{K})$ (throughout this paper, we suppress Boltzmann constant, implying the conversion 1 keV = 1.16045 × 10^7 K). At $\beta_{\mathrm{p}} \gg 1$ we have $\tilde{\Lambda}^{(\mathrm{pe})}_{10} \sim 1$ (and $\tilde{\Lambda}^{(\mathrm{pe})}_{10} \sim \beta_{\mathrm{p}}^{1/2}|\ln\beta_{\mathrm{p}}|$ for $\beta_{\mathrm{p}} \ll 1$ (see Section 3.1). The collisional excitation rate is $\Gamma^{C(\mathrm{pe})}_{01} = \Gamma^{C(\mathrm{pe})}_{10}\exp(-\beta_{\mathrm{p}})$. The contribution to Landau excitation from proton–proton collisions is of similar order and will be neglected in this section.

(ii) **Radiative Transitions.** The spontaneous decay rate of the first Landau level is

$$\Gamma^{A}_{10} = \frac{4}{3}\frac{e^2\omega_{\mathrm{cp}}^2}{m_{\mathrm{p}}c^3}. \tag{5}$$

We neglect here the radiative absorption and stimulated emission.

(iii) **Statistical equilibrium.** The relative population of protons in $N = 0$ and $N = 1$ is determined by

$$n_1/n_0 = \mathrm{e}^{-\beta_{\mathrm{p}}}\left[1 + \Gamma^{A}_{10}/\Gamma^{C}_{10}\right]^{-1}, \tag{6}$$

When $\Gamma^{A}_{10}/\Gamma^{C}_{10} \ll 1$, the Boltzmann distribution (i.e. LTE) is recovered, $n_1 = \mathrm{e}^{-\beta_{\mathrm{p}}} n_0$. In this case, the cyclotron absorption and emission are related by the Kirchhoff law.

In the opposite case $\Gamma^{C}_{10}/\Gamma^{A}_{10} \ll 1$, we have $n_1/n_0 = \Gamma^{C}_{01}/\Gamma^{A}_{10}$, i.e. collisional excitation ($0 \to 1$) is balanced by radiative decay ($1 \to 0$).

With $n_{\mathrm{e}} = \rho/m_{\mathrm{p}}$, we see that

$$\Gamma^{C(\mathrm{pe})}_{10}/\,\Gamma^{A}_{10} = 28.6\,\rho_0\,B_{14}^{-7/2}\,\tilde{\Lambda}^{(\mathrm{pe})}_{10}. \tag{7}$$

The ratio (7) is larger than unity for ordinary neutron star atmospheres, but it can become smaller than unity for magnetars.

The above situation should be contrasted with that of electrons. The deexcitation rate of an electron from its first excited Landau level to the ground state due to collisions with protons (treated as classical particles) is of the order of $4\sqrt{2\pi}n_{\mathrm{p}}a_{\mathrm{m}}^3 e^4 m_{\mathrm{e}}/\hbar^3$ for $\beta_{\mathrm{e}} = \hbar\omega_{\mathrm{ce}}/T \gg 1$ [cf. equation (4)]. The spontaneous cyclotron decay rate of electron is $\Gamma^{A}_{10}(e) = 4e^2\omega_{\mathrm{ce}}^2/(3m_{\mathrm{e}}\,c^3)$, and the ratio Γ^C/Γ^A is about a factor $(m_{\mathrm{e}}/m_{\mathrm{p}})^{7/2}$ smaller than that for protons. Thus for electrons, radiative deexcitation is always much faster than collisional deexcitation, and there is no true electron cyclotron absorption, but only scattering, in the magnetic fields of ordinary pulsars and magnetars.

3 NON-RADIATIVE COULOMB COLLISION RATES

Coulomb collision rates of non-degenerate fermions in a strong magnetic field have been studied by many authors. Ventura (1973) derived collision rates for electrons scattered by a fixed Coulomb potential. Pavlov & Yakovlev (1976) presented transition probabilities for collisions of two non-relativistic particles, which interact via a screened Coulomb potential. As a particular case they recovered the result of Ventura (1973), but in a simpler form. Relativistic expressions for Coulomb collision rates of non-degenerate fermions in a magnetic field were derived by Langer (1981) and Storey & Melrose (1987). However, since we are interested in Landau transitions of ions, we may take the non-relativistic approach (Pavlov & Yakovlev 1976). Accordingly, we do not consider Coulomb spin-flip transitions which generally are weaker by a factor $\sim b_\mathrm{i}$ compared to the transitions which preserve spin. The spin distribution, however, may affect statistical equilibrium through exchange effects.

3.1 Proton–electron collisions

General formulae for Coulomb collision rates of two different particles with arbitrary charges are given in Appendix A2.1. Here we consider electron collisions with protons, assuming that the electrons remain in the ground Landau state. This particular case has been previously considered by Miller, Salpeter & Wasserman (1987), based on Pavlov & Yakovlev (1976). For a given relative velocity (along z) v_z between a proton and an electron, the transition rate from proton Landau level N to N' is

$$W_{NN'}^{(\mathrm{pe})}(v_z) \equiv n_\mathrm{e} v_z \sigma_{NN'}^{(\mathrm{pe})}(v_z) = 4\pi\tau_0^{-1} n_\mathrm{e} a_\mathrm{m}^3 \sum_{\pm} w_{NN'}^{(\mathrm{pe})}(u_\pm)/u', \tag{8}$$

where $\sigma_{NN'}^{(\mathrm{pe})}(v_z)$ is the corresponding cross-section, $\tau_0 = \hbar^3/(e^4 m_\mathrm{e}) = 2.42 \times 10^{-17}$ s is the atomic unit of time, n_e is the electron number density, and

$$w_{NN'}^{(\mathrm{pe})}(u_\pm) = \int_0^\infty \frac{\mathrm{e}^{-t/2} I_{NN'}^2(t/2)}{(t+u_\pm^2)^2}\,\mathrm{d}t. \tag{9}$$

Here $u_\pm^2 = (u \pm u')^2 + u_\mathrm{s}^2$, and $u = (m_*|v_z|/\hbar)\, a_\mathrm{m}$ and $u' = (m_*|v_z'|/\hbar)\, a_\mathrm{m}$ are scaled relative velocities along z, which satisfy the energy conservation law $u'^2 = u^2 + 2(N-N')m_*/m_\mathrm{p}$, where $m_* = m_\mathrm{e} m_\mathrm{p}/(m_\mathrm{e}+m_\mathrm{p})$ is the reduced mass. The parameter $u_\mathrm{s} = k_\mathrm{s} a_\mathrm{m}$, included in $u_\pm$, is the scaled Debye screening wave number (k_s^{-1} is the Debye screening length). For a neutral electron–proton plasma at temperature T we have $k_\mathrm{s} = \sqrt{8\pi n_\mathrm{e} e^2/T} = (1.584 \times 10^8\ \mathrm{cm}^{-1})\rho_0^{1/2} T_6^{-1/2}$. Equations (8) and (8) follow from (A19) and (A20) of Appendix A with $Z_1 = Z_2 = 1$ and $w_{NN'}^{(\mathrm{pe})}(u_\pm) = w_{0,N;0,N'}(u_\pm)$. Laguerre function $I_{NN'}$ is defined by equation (A4).

If the distributions of z-velocities of electrons and protons are Maxwellian with temperatures T_e and T_p, respectively, which do not depend on the Landau number N, then the relative velocities $v_z = \hbar k/m_*$ have Maxwellian distribution

$$\mathcal{F}_{m_*,T}(v_z) = \sqrt{\frac{m_*}{2\pi T}}\, \exp\left(-\frac{m_* v_z^2}{2T}\right), \tag{10}$$

where

$$T = (m_\mathrm{e}+m_\mathrm{p})/\left(m_\mathrm{e} T_\mathrm{p}^{-1} + m_\mathrm{p} T_\mathrm{e}^{-1}\right). \tag{11}$$

In order to simplify formulae, hereafter we assume $T_\mathrm{e} = T_\mathrm{p} = T$, unless the opposite is explicitly stated. Then the velocity-averaged partial Coulomb transition rate $n_\mathrm{e}\langle v_z \sigma_{NN'}^{(\mathrm{pe})}\rangle$ is

$$\Gamma_{NN'}^{C(\mathrm{pe})} = 4(e^4/\hbar^2)\sqrt{2\pi m_*/T}\, n_\mathrm{e} a_\mathrm{m}^2 \Lambda_{NN'}^{(\mathrm{pe})} \tag{12a}$$

$$= \frac{4\sqrt{2\pi}}{\tau_0}\left(\frac{m_* m_\mathrm{p}}{m_\mathrm{e}^2}\right)^{1/2} n_\mathrm{e} a_\mathrm{m}^3 \tilde{\Lambda}_{NN'}^{(\mathrm{pe})}, \tag{12b}$$

where

$$\tilde{\Lambda}_{NN'}^{(\mathrm{pe})} = \sqrt{\beta_\mathrm{p}}\, \Lambda_{NN'}^{(\mathrm{pe})}, \tag{13a}$$

$$\Lambda_{NN'}^{(\mathrm{pe})} = \int_0^\infty \frac{\mathrm{d}u}{u'}\, \mathrm{e}^{-\beta_* u^2/2}\, \theta(u'^2)\, g(u) g(u') \times \left[w_{NN'}^{(\mathrm{pe})}(u_+) + w_{NN'}^{(\mathrm{pe})}(u_-)\right]. \tag{13b}$$

Here $\theta(u'^2)$ [with $u'^2 \equiv u^2 + 2(N-N')m_*/m_\mathrm{p}$] is the step function that ensures the energy conservation, $\beta_* \equiv \hbar eB/m_* cT = \beta_\mathrm{p} m_\mathrm{p}/m_*$, and $g(u)g(u')$ is the correction factor, which approximately allows for violation of Born approximation as discussed in Appendix A1.4. The latter factor appreciably differs from 1 only at $u \lesssim \gamma_B^{-1/2}$, where $\gamma_B = \hbar^3 B/(m_*^2 ce^3)$. In the case of electron–proton collisions $\gamma_B^{-1/2} \approx \alpha_\mathrm{f}/\sqrt{b_\mathrm{e}} = 0.004848\, B_{14}^{-1/2}$. The smallness of $\gamma_B^{-1/2}$ ensures that the approximations used to derive equation (13b) are sufficiently accurate; in this case the γ_B-dependence in equation (13b) is weak (logarithmic).

By changing integration variable $u \to u'$ in equation (13b), and taking into account that $w_{NN'}^{(\mathrm{pe})}(u_\pm) = w_{N'N}^{(\mathrm{pe})}(u_\pm)$, we can check that $\Lambda_{NN'}^{(\mathrm{pe})} = \mathrm{e}^{\beta_\mathrm{p}(N-N')} \Lambda_{N'N}^{(\mathrm{pe})}$, and thus

$$\Gamma_{NN'}^{C(\mathrm{pe})} = \mathrm{e}^{\beta_\mathrm{p}(N-N')} \Gamma_{N'N}^{C(\mathrm{pe})}. \tag{14}$$

Fig. 1 depicts the function $\Lambda_{NN'}^{(\mathrm{pe})}$ ($N > N'$) for transitions between different low-lying proton Landau states, calculated assuming $u_\mathrm{s} \to 0$ and $\gamma_B^{-1} \to 0$. Fig. 2 presents the same functions for $u_\mathrm{s} = 0.5$. Note that $u_\mathrm{s} = k_\mathrm{s} a_\mathrm{m} = 4.1 \times 10^{-3} \rho_0^{1/2} T_6^{-1/2} B_{14}^{-1/2}$. So $u_\mathrm{s} = 0.5$ corresponds to a rather high plasma density. We see that at any B and u_s transitions between neighbouring states ($N - N' = 1$) strongly dominate.

Representation (12b) is most convenient when $\beta_\mathrm{p} \gg 1$, because in this case the exponential function in equation (13b) varies much faster than u' and $w_{NN'}^{(\mathrm{pe})}$, and it can be integrated separately. Hence $\tilde{\Lambda}_{NN'}^{(\mathrm{pe})}$ approaches a constant.

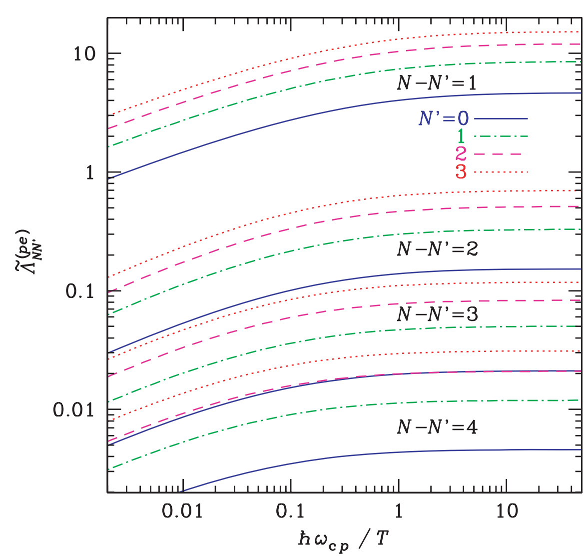

Figure 1. The dimensionless quantity $\tilde{\Lambda}_{NN'}^{(\mathrm{pe})}$ (equation 13b) as a function of $\beta_\mathrm{p} = \hbar\omega_\mathrm{cp}/T$ for transitions between several lowest proton Landau states for screening parameter $u_\mathrm{s} = 0$.

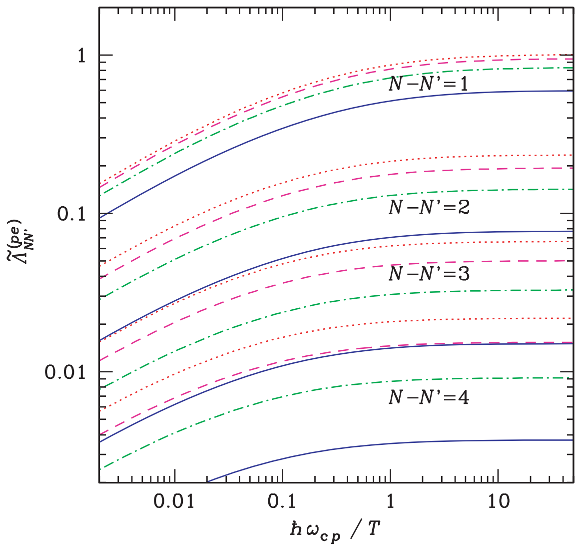

Figure 2. The same as in Fig. 1, but for screening parameter $u_{\rm s} = 0.5$.

In the opposite limit $\beta_{\rm p} \ll 1$ it may be more convenient to use equation (12a), because in this case $\Lambda^{\rm (pe)}_{NN'}$ is a slowly varying function of $\beta_{\rm p}$. At the first glance it may seem unphysical that equation (12a) contains factor $a_{\rm m}^2$ which goes to infinity as B goes to zero. However, it has a simple explanation. As long as the Landau numbers of the electron (equal to zero) and proton (N, N') are kept fixed, equation (12a) describes the partial rate of the collisions in which the transfer of the kinetic energy of the motion transverse to the field, $|N - N'|\hbar\omega_{\rm cp}$, decreases linearly with decreasing B. In the classical picture this corresponds to collisions with impact parameters increasing $\propto a_{\rm m}$, for which the cross-section increases according to the Rutherford formula. The divergence of the classical cross-section at large impact parameters is eliminated if one takes into account the screening of the Coulomb potential. It is also the case for the quantum cross-section. Indeed, $u_\pm^2$ in the denominator of equation (8) in general includes the term $u_{\rm s}^2 = k_{\rm s}^2\, a_{\rm m}^2$. Thus $w^{\rm (pe)}_{NN'}(u_\pm)$ (and hence $\Lambda^{\rm (pe)}_{NN'}$) becomes $\propto (k_{\rm s} a_{\rm m})^{-4}$ when the magnetic length $a_{\rm m}$ is much larger than the screening length $k_{\rm s}^{-1}$.

3.2 Proton–proton collisions

Now let us consider proton–proton collisions. This case is more complicated than the previous one in two respects: first, there is the exchange interaction described in Appendix A2.2, and secondly, both colliding particles can change their Landau numbers (neither of them is confined to the ground state).

Let n_N be the number density of protons in the Nth Landau state, and let $f_N^\uparrow$ and $f_N^\downarrow$ be the fraction of such protons with spin along and opposite to the field direction, respectively ($f_N^\uparrow + f_N^\downarrow = 1$). Then the average rate of proton transitions from level N to level N' due to the Coulomb collisions is

$$\Gamma^{C\rm (pp)}_{NN'} = \frac{1}{2}\sum_{N_2 N_2'} n_{N_2}\Big[\big(f_N^\uparrow f_{N_2}^\downarrow + f_N^\downarrow f_{N_2}^\uparrow\big)\,\big\langle v_z\sigma^{\rm (pp)+}_{NN_2;N'N_2'}\big\rangle + \big(f_N^\uparrow f_{N_2}^\uparrow + f_N^\downarrow f_{N_2}^\downarrow\big)\,\big\langle v_z\sigma^{\rm (pp)-}_{NN_2;N'N_2'}\big\rangle\Big], \qquad (15)$$

where $\langle v_z\sigma^{\rm (pp)\pm}_{NN_2;N'N_2'}\rangle$ is the probability, per unit time, that two protons in unit volume, which have initial Landau numbers N and N_2, make a transition to the state where they have Landau numbers N' and N'_2, under the condition that their spin projections to $\boldsymbol{B}$ are the same (sign −) or opposite (sign +). The factor $\frac{1}{2}$ at the sum allows for the quantum statistics of identical particles.

For Maxwell distribution (10) with $m_* = m_{\rm p}/2$, using the results of Appendix A2, we obtain

$$\big\langle v_z\sigma^{\rm (pp)\pm}_{NN_2;N'N_2'}\big\rangle = 8\,(e^4/\hbar^2)\,\sqrt{\pi m_{\rm p}/T}\,a_{\rm m}^2 \times \int_0^\infty \frac{{\rm d}u}{u'}\,{\rm e}^{-\beta_{\rm p}u^2}\Big[w_{NN_2;N'N_2'}(u_+) + w_{NN_2;N'N_2'}(u_-) \pm 2\,w^x_{NN_2;N'N_2'}(u_-,u_+)\Big], \qquad (16)$$

where $u_\pm^2 = (u \pm u')^2 + u_{\rm s}^2$ and $u' = [u^2 + N' - N + N'_2 - N_2]^{1/2}$. Functions $w_{NN_2;N'N_2'}$ and $w^x_{NN_2;N'N_2'}$ are given by equations (A20) and (A24), respectively.

Equations (15) and (16) can be written in the form analogous to equation (12b),

$$\Gamma^{C\rm (pp)}_{NN'} = \sum_{N_2} n_{N_2}\big\langle v_z\sigma^{(N_2)}_{NN'}\big\rangle, \qquad (17)$$

$$\big\langle v_z\sigma^{(N_2)}_{NN'}\big\rangle = 4\sqrt{\pi}\,\frac{a_{\rm m}^3}{\tau_0}\,\frac{m_{\rm p}}{m_{\rm e}}\Big[\tilde\Lambda^{\rm (pp)}_{NN_2;N'} - \big(f_N^\uparrow - f_N^\downarrow\big)\big(f_{N_2}^\uparrow - f_{N_2}^\downarrow\big)\,\tilde\Lambda^{({\rm pp},x)}_{NN_2;N'}\Big], \qquad (18)$$

where

$$\tilde\Lambda^{\rm (pp)}_{NN_2;N'} = \sqrt{\beta_{\rm p}}\sum_{N_2'}\int_0^\infty \frac{{\rm d}u}{u'}\,{\rm e}^{-\beta_{\rm p}u^2}\,\theta(u'^2)\,g(u)g(u') \times\big[w_{NN_2;N'N_2'}(u_+) + w_{NN_2;N'N_2'}(u_-)\big], \qquad (19a)$$

$$\tilde\Lambda^{({\rm pp},x)}_{NN_2;N'} = 2\sqrt{\beta_{\rm p}}\sum_{N_2'}\int_0^\infty \frac{{\rm d}u}{u'}\,{\rm e}^{-\beta_{\rm p}u^2}\,\theta(u'^2)\,g(u)g(u') \times w^x_{NN_2;N'N_2'}(u_-,u_+). \qquad (19b)$$

In these equations u' and $u_\pm$ depend on N'_2. The factors $g(u)g(u')$, with $g(u)$ defined by equation equation (A16), account for the correction due to violation of Born approximation, as discussed in Appendix A1.4. However, unlike Section 3.1, here $\gamma_B^{-1/2} = \alpha_{\rm f} m_{\rm p}/(2m_{\rm e}\sqrt{b_{\rm e}}) = 4.45\,B_{14}^{-1/2}$ is larger than 1 for $B < 2\times10^{15}$ G, which reflects the fact that the protons are moving much slower than the electrons, therefore Born and adiabatic approximations (see Appendix A1.4) are less applicable to the proton–proton collisions. Nevertheless, we use these approximations, considering them as order-of-magnitude estimates, which is justified because the whole effect of the proton–proton collisions on statistical equilibrium is not very significant, as we will see below.

In Fig. 3 we show $\tilde\Lambda^{\rm (pp)}_{NN_2;N'}$ for the case of negligible screening ($u_{\rm s} = 0$) and $\gamma_B = 1$, for a few initial and final proton Landau numbers N, N', and for initial Landau numbers of the second proton $N_2 = 0$, 1, 2. The decrease of the displayed functions at $\beta_{\rm p} \gg 1$ results from the correction beyond Born approximation. This indicates that an accurate evaluation of the proton–proton collision rates would require non-Born quantum calculations, which are beyond the scope of the present paper.

In Fig. 4 we compare some of the curves from Fig. 3 (solid lines) with the case of non-negligible screening, $k_{\rm s}a_{\rm m} = u_{\rm s} = 0.5$ (dot-dashed lines), which can be relevant at rather high density. Also in this figure we show a comparison of $\tilde\Lambda^{\rm (pp)}_{NN_2;N'}$ (solid lines) with the difference $\tilde\Lambda^{\rm (pp)}_{NN_2;N'} - \tilde\Lambda^{({\rm pp},x)}_{NN_2;N'}$ (dashed lines) which enters equation equation (18) when the proton spins are all aligned in the same direction.

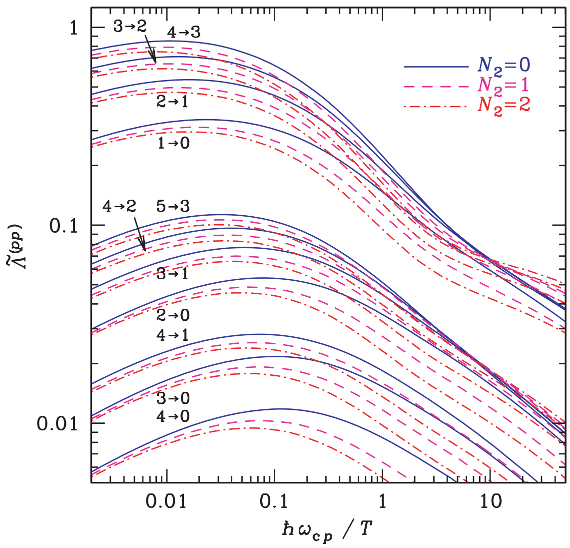

Figure 3. The dimensionless function $\tilde\Lambda^{(\mathrm{pp})}_{NN_2;N'}$ (equation 19a) without screening ($u_\mathrm{s}=0$) for the transitions between the proton Landau states marked near the curves. Initial Landau number of the second proton equals $N_2=0$ (solid lines), $N_2=1$ (dashed lines) or $N_2=2$ (dot–dashed lines).

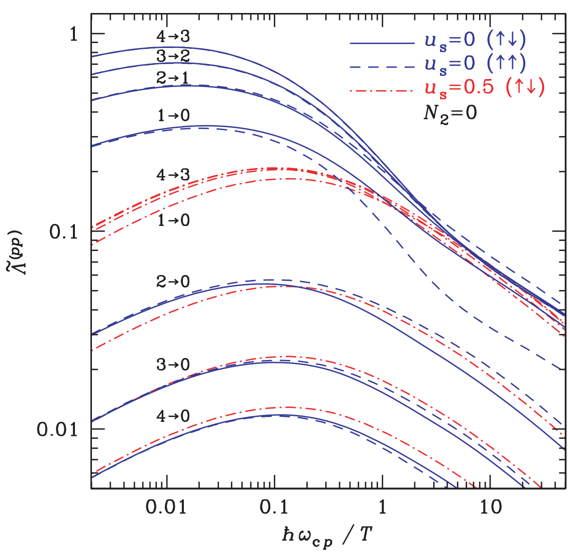

Figure 4. The functions $\tilde\Lambda^{(\mathrm{pp})}_{NN_2;N'}$ (solid lines without screening and dot–dashed lines with screening parameter $u_\mathrm{s}=0.5$) and $\tilde\Lambda^{(\mathrm{pp})}_{NN_2;N'}-\tilde\Lambda^{(\mathrm{pp},x)}_{NN_2;N'}$ (dashed lines, without screening), representing the expression in the square brackets of equation equation (18) for random spin orientations ($f^\uparrow=f^\downarrow=0.5$) and for aligned spins ($f^\uparrow=1$), respectively, for transitions $N\to N-1$ and $N\to 0$, with $N=1, 2, 3, 4$, $N_2=0$, as functions of $\beta_\mathrm{p}=\hbar\hbar\omega_\mathrm{cp}/T_\mathrm{p}$.

Let us note that if $T_\mathrm{e}\neq T_\mathrm{p}$, then in this section T_p should substitute T defined by equation (11). In particular, $\beta_\mathrm{p}=\hbar\omega_\mathrm{cp}/T_\mathrm{p}$ in equations (16) and (19).

4 RADIATIVE TRANSITIONS

4.1 Radiative transition rates in magnetized plasmas

Magnetized plasma is a birefringent medium. Electromagnetic radiation propagates through it in the form of two normal polarization modes $j=1, 2$ with polarization vectors $\boldsymbol{e}^j(\omega,\mathbf{n})$ (e.g. Ginzburg 1970). Here, ω is the angular frequency and $\mathbf{n}$ the unit vector along the wave vector. Consequently, radiative transition rates depend not only on ω, but also on j and $\mathbf{n}$.

Let $\Gamma^A_{NN'}$, $\Gamma^B_{NN'}$, and $\hat\Gamma^B_{NN'}$ be the rates of transitions from level N to N' due to spontaneous emission, photoabsorption, and stimulated emission, respectively.[1] These rates are the *total* (for both polarizations, integrated over angles and frequencies) transition probabilities per unit time for one occupied initial quantum state. They can be expressed through Einstein coefficients $A_{NN'}$ and $\hat B_{NN'}$ (for emission), or $B_{NN'}$ (for absorption). These coefficients have different definitions in the literature (e.g. cf. Rybicki & Lightman 1979; Ginzburg 1970; Zheleznyakov 1996). We define $A_{NN'}$, $B_{NN'}$, and $\hat B_{NN'}$ from the conditions that the number of quanta with angular frequencies in the interval d ω and wave vectors in solid angle element d $\mathbf{n}$ spontaneously emitted by a unit volume during unit time equals $n_N A_{NN'}\,\mathrm{d}\omega\,\mathrm{d}\mathbf{n}$, and the number of quanta emitted or absorbed under the action of radiation with the specific intensity I_ω equals $n_N\hat B_{NN'}I_\omega\,\mathrm{d}\omega\mathrm{d}\mathbf{n}$ or $n_N B_{NN'}I_\omega\,\mathrm{d}\omega\mathrm{d}\mathbf{n}$, respectively (Zheleznyakov 1996). This definition (or a similar one in Ginzburg 1970, but not the one in Rybicki & Lightman 1979) is relevant in a strong magnetic field, where the emission is neither isotropic, nor unpolarized. Then

$$\Gamma^B_{NN'}=\sum_{j=1,2}\int\mathrm{d}\mathbf{n}\int\mathrm{d}\omega B_{NN'}(j,\omega,\mathbf{n})\,I_{\omega,j}(\mathbf{n}),\tag{20}$$

$$\Gamma^A_{NN'}=\sum_{j=1,2}\int\mathrm{d}\mathbf{n}\int\mathrm{d}\omega\,A_{NN'}(j,\omega,\mathbf{n}),\tag{21}$$

and the expression for $\hat\Gamma^B_{NN'}$ is completely analogous to equation equation (20).

The quantities $A_{NN'}$, $\hat B_{NN'}$ and $B_{N'N}$ are related by the Einstein relations (which include polarization dependence, see, e.g. Ginzburg 1970; Zheleznyakov 1996):[2]

$$\hat B_{NN'}=B_{N'N},\qquad A_{NN'}=\frac{\hbar\omega^3}{8\pi^3c^2}\,B_{N'N}.\tag{22}$$

From the first of these relations, it follows that the stimulated emission rate is equal to that of photoabsorption with interchange of the initial and final levels: $\hat\Gamma^B_{NN'}=\Gamma^B_{N'N}$.

In equation (22) we have neglected the difference of the group and phase velocities of radiation. Einstein relations with allowance for this difference are given, e.g. by Ginzburg (1970) and Zheleznyakov (1996). Note, however, that this difference would lead to appearance of additional factors not only in equation (22), but also in the expressions for photoabsorption cross-sections discussed in Section 4.2 below.

Spontaneous cyclotron decay rates have been derived by Daugherty & Ventura (1977) (see also Daugherty & Ventura 1978; Melrose & Zheleznyakov 1981; Pavlov et al. 1991; Baring, Gonthier & Harding 2005, and references therein). In the non-relativistic limit ($Nb_\mathrm{i}\ll 1$), the decay rates are proportional to $b_\mathrm{i}^{N-N'+1}$, multiplied by a combinatorial factor. Although the latter factor may be large for large $N'-N$, transitions $N\to N'=N-1$ still dominate in

[1] Generally, N and N' may take any values. For instance, free–free photoabsorption is allowed for $N'\leqslant N$ (i.e. the photon is absorbed while the proton makes a downward transition) as well as for $N'>N$.

[2] Einstein relations (22) come from the detailed balance equation $n_{N'}B_{N'N}I_{\omega,j}=n_NA_{NN'}+n_N\hat B_{NN'}I_{\omega,j}$ in the complete thermodynamic equilibrium, where $I_{\omega,j}=\frac{1}{2}B_\omega=(\hbar\omega^3/8\pi^3c^2)\,(\mathrm{e}^{\hbar\omega/T}-1)^{-1}$, and the requirement that the coefficients A and B must be independent of T.

the non-relativistic regime. The rates of the latter transitions are $\Gamma^A_{N,N-1} = N\Gamma_{\rm r,p}$, where

$$\Gamma_{\rm r,p} = \frac{4}{3}\,\frac{e^2\omega_{\rm cp}^2}{m_{\rm p}\,c^3} \tag{23}$$

is the natural width of the proton cyclotron line.

Spin-flip transitions for protons are unimportant in the non-relativistic limit, because their rates contain an additional factor $b_{\rm i}$ compared to the dominant transitions preserving spin (e.g. cf. Melrose & Zheleznyakov 1981).

4.2 Relation between emission rates and photoabsorption cross-sections

The Einstein absorption coefficient $B_{NN'}$ is given by the relation

$$B_{NN'}(j,\omega,\mathbf{n}) = \sigma_{NN'}(j,\omega,\mathbf{n})/\hbar\omega, \tag{24}$$

where $\sigma_{NN'}$ is the partial photoabsorption cross-section responsible for the $N \rightarrow N'$ transition. Equation (24) directly follows from the definition of $B_{NN'}$ in Section 4.1. Together with Einstein relations, it allows one to express spontaneous decay rates $\Gamma^A_{NN'}$ through partial photoabsorption cross-sections.

In the 'rotating coordinates' (e.g. Mészáros 1992), the polarization vectors $\boldsymbol{e}^j(\omega,\mathbf{n})$ of two polarization modes $j = 1, 2$ have the components e^j_α, $\alpha = 0, \pm 1$. In the dipole approximation, photoabsorption cross-sections can be written as (e.g. Ventura, Nagel & Mészáros 1979)

$$\sigma(j,\omega,\mathbf{n}) = \sum_{\alpha=-1}^{1} \sigma_\alpha(\omega)\,\left|e^j_\alpha(\omega,\mathbf{n})\right|^2, \tag{25}$$

where the component e_- is responsible for the electron cyclotron resonance, and e_+ for the ion cyclotron resonance.

Using equations (21), (22) and (24), one obtains

$$\Gamma^A_{N'N} = \sum_{j=1,2} \int \mathrm{d}\mathbf{n} \int \frac{\omega^2 \mathrm{d}\omega}{8\pi^3 c^2}\,\sigma_{NN'}(j,\omega,\mathbf{n}). \tag{26}$$

As already stated in Section 4.1, we neglect the difference of the group and phase velocities of radiation. This is equivalent to the 'semi-transverse approximation' (Ventura 1979), where refraction indices are close to 1, and $\mathbf{n}\cdot\boldsymbol{e}^j \approx 0$. In this approximation, the relation $\sum_{j=1,2} A^j_\alpha = 1$ holds, where

$$A^j_\alpha \equiv \frac{3}{8\pi}\int \left|e^j_\alpha(\omega,\mathbf{n})\right|^2 \mathrm{d}\mathbf{n}. \tag{27}$$

Then equations (25) and (26) give

$$\Gamma^A_{N'N} = \sum_\alpha \int \frac{\omega^2\,\mathrm{d}\omega}{3\pi^2\,c^2}\,\sigma_{\alpha,NN'}(\omega). \tag{28}$$

Let us suppose that transition $N \rightarrow N'$ corresponds to an absorption line with a profile $\phi(\omega)(\int\phi(\omega)\mathrm{d}\omega = 1)$, which at $\omega = \omega_0$ has a sharp peak with a characteristic half-width $\nu \ll \omega_0$ for the polarization α. At $\omega \sim \omega_0$, let us write the photoabsorption cross-section in the form $\sigma_{\alpha,NN'}(\omega) = 2\nu\bar{\sigma}_{\alpha,NN'}\phi(\omega)$. Then equation (28 gives the spontaneous emission rate

$$\Gamma^A_{N'N} \approx \frac{2\nu\bar{\sigma}_{\alpha,NN'}\,\omega_0^2}{3\pi^2 c^2}. \tag{29}$$

Let us assume, in addition, that $I_{\omega,j}(\mathbf{n})$ can be replaced by the average over the angles under the integral in equation (20, which we denote $\bar{I}_{\omega,j}$ (this replacement is exact in the diffusion approximation). Then, using equations (24) and (27), we obtain the photoabsorption and stimulated emission rates

$$\Gamma^B_{NN'} = \hat{\Gamma}^B_{N'N} = \frac{8\pi^3 c^2}{\hbar\omega_0^3}\,\Gamma^A_{N'N}\sum_{j=1,2} A^j_\alpha\,J_j, \tag{30}$$

where

$$J_j \equiv \int \bar{I}_{\omega,j}\,\phi_j(\omega)\,\mathrm{d}\omega. \tag{31}$$

4.3 Cross-sections at the proton cyclotron resonance

Although cyclotron emission rates can be calculated in the framework of the first-order perturbation theory, this theory is not suitable for the determination of the frequency dependence of photoabsorption cross-sections and opacities. The reasons for that, and the conditions where the first-order process still can be important, were discussed by Daugherty & Ventura (1978), who stressed that the spectral dependence of the absorption coefficient is properly described by second- and higher-order processes. Indeed, because of kinematic requirements (energy and momentum conservation), the first-order absorption is possible only at a single frequency at any given angle of incidence. Thus one must take into account level broadening in order to obtain the spectral absorption coefficient. The broadening is caused by the finite life time of the proton in a final state after an absorption event. In a macroscopically homogeneous plasma this life time is limited only by (1) spontaneous emission and (2) interactions with other particles. It is the emitted photon in the first case or another plasma particle in the second case that carries the energy and momentum needed to restore the kinematic balance. Thus a quantum description of the absorption line shape requires at least two-vertex Feynman diagrams. The second vertex may correspond to the emission of the photon [case (1); cf. Figs 1 and 2 of Daugherty & Ventura 1978] or to Coulomb interaction with a charged particle [case (2)]. The first case is scattering, and the second is free–free photoabsorption. We now consider the cross-sections for these two processes for the polarization component $\alpha = +1$, corresponding to the proton cyclotron resonance.

4.3.1 Free–free absorption

The free–free photoabsorption cross-section at any frequencies and polarizations is given by equations (B1)–(B3) of Appendix B. It can be presented as a sum of terms corresponding to transitions of a proton from level N to N':

$$\sigma^{\rm ff}_\alpha(\omega) = \sum_N f^{\rm p}_N \sum_{N'} \sigma^{\rm ff}_{\alpha,NN'}(\omega), \tag{32}$$

where $f^{\rm p}_N$ is the fraction of protons in Landau state N, and

$$\sigma^{\rm ff}_{\alpha,NN'}(\omega) = \frac{4\pi e^2}{m_{\rm e}c}\,\frac{\omega^2\sum_n f^{\rm e}_n \sum_{n'}\nu^{\rm ff,\alpha}_{n,N;n',N'}(\omega)}{(\omega+\alpha\omega_{\rm ce})^2(\omega-\alpha\omega_{\rm cp})^2+\omega^2\tilde{\nu}^2_\alpha(\omega)}, \tag{33}$$

where $f^{\rm e}_n$ is the fraction of the electrons in Landau state n, and $\tilde{\nu}_\alpha(\omega)$ is a damping factor. The separation of $\sigma^{\rm ff}_\alpha$ into $\sigma^{\rm ff}_{\alpha,NN'}$, expressed by equation (32), is useful for calculation of non-LTE emissivity (see Section 6).

At $\omega \sim \omega_{\rm cp}$ and $\alpha = +1$, there is a resonance:

$$\sigma^{\rm ff}_+(\omega) \approx \frac{4\pi e^2}{m_{\rm p}c}\,\frac{\nu^{\rm ff}_{\rm p}}{(\omega-\omega_{\rm cp})^2+\nu^2}, \tag{34}$$

where $\nu = (m_{\rm e}/m_{\rm p})\tilde{\nu}_+(\omega_{\rm cp}) = \hat{\nu}_{\rm p} + \nu^{\rm ff}_{\rm p}$, with $\hat{\nu}_{\rm p} = \nu_{\rm p}(\omega_{\rm cp})$ the radiative damping rate $\Gamma_{\rm r,p}/2$ (note that it could also include other damping mechanisms not related to electron–proton collisions, such as the damping rate due to collisions with neutral particles), and $\nu_{\rm p}^{\rm ff}$ the damping rate due to electron–proton collisions:

$$\nu_{\rm p}^{\rm ff} = (m_{\rm e}/m_{\rm p})\, \nu_{+}^{\rm ff}(\omega_{\rm cp}), \tag{35}$$

with $\nu_{+}^{\rm ff}$ (ω) given by equation (B2). From equation (28), taking into account the condition $\nu \ll \omega_{\rm cp}$, we obtain the rate of $N' \to N$ transitions caused by the resonant free–free emission,

$$\Gamma^{\rm ff}_{+,N'N} \approx \frac{4\sqrt{2\pi}}{\tau_0}\left(\frac{m_{\rm p}}{m_{\rm e}}\right)^{1/2} n_{\rm e} a_{\rm m}^3 \times \frac{\sqrt{\beta_{\rm p}}}{3\pi}\int \frac{\Gamma_{\rm r,p}\,\Lambda^{\rm ff,+1}_{0,N;0,N'}}{(\omega-\omega_{\rm cp})^2+\nu^2}\,{\rm d}\omega, \tag{36}$$

where $\Lambda^{\rm ff,+1}_{n,N;n',N'}$ is given by equation (B10). This result is written in the form similar to equation (12b) for easy comparison, which shows that by order of magnitude $\Gamma^{\rm ff}/\,\Gamma^{C(\rm pe)} \sim \Gamma_{\rm r,p}/\nu$. The damping factor ν is discussed in Section 4.3.2; here we note only that the ratio $\Gamma^{\rm ff}/\,\Gamma^{C(\rm pe)}$ cannot be large, because $\nu \geqslant \Gamma_{\rm r,p}/2$.

4.3.2 Scattering

The resonant cyclotron scattering (Canuto, Lodenquai & Ruderman 1971; Ventura 1979) is a second-order process which is common for electrons in white dwarfs and magnetic neutron stars, and for ions in magnetars. The photon-proton scattering cross-section is

$$\sigma_{+}^{\rm sc} = \sigma_{\rm Tp}\,\frac{\omega^2}{(\omega-\omega_{\rm cp})^2+\nu^2}, \tag{37}$$

where $\sigma_{\rm Tp} = 8\pi e^4/(3m_{\rm p}^2c^4)$ is the Thomson cross-section for protons.

The determination of the effective damping factor ν (not considered by Canuto et al. 1971) is not trivial. In general, this task requires a non-perturbative treatment (Cohen-Tannoudji, Dupont-Roc & Grynberg 1998), which goes beyond the scope of our paper. However, $\nu(\omega)$ can be found from the correspondence to the classical physics.

The naıve estimate of ν as the sum of total half-widths of two Landau levels would lead to replacement of equation (37) by a sum of different Lorentz profiles for different proton states N. However, this estimate is incorrect, because it ignores the coherence of equally spaced quantum states, as discussed, e.g. by Cohen-Tannoudji et al. (1998) for the case of interaction of electromagnetic field with a quantum oscillator. Interference of transition amplitudes between different states leads to the common damping factor (which proves to be equal to the classical oscillator damping factor) for all transitions which have the same resonant frequency. Thus we should put in equation (37) the same damping factor as in equation (35), $\nu = \hat{\nu}_{\rm p} + \nu_{\rm p}^{\rm ff}$ at $\omega \approx \omega_{\rm cp}$. The frequency dependence of ν is suggested by analogy with a classical oscillator (Jackson 1975):

$$\nu(\omega) = \nu_{\rm p}(\omega) + (m_{\rm e}/m_{\rm p})\,\nu_{+}^{\rm ff}(\omega), \tag{38}$$

with

$$\nu_{\rm p}(\omega) = \frac{2}{3}\,\frac{e^2}{m_{\rm p}c^3}\,\omega^2. \tag{39}$$

Thus we recover the damping factor that was previously given without discussion by Pavlov et al. (1995). Obviously, at the resonance, $\nu_{\rm p}(\omega_{\rm cp}) = \hat{\nu}_{\rm p} = \Gamma_{\rm r,p}/2$.

Note that for damping of free–free photoabsorption (equation [B3]) we should include, beside $\nu_{\rm p}(\omega)$, also $\nu_{\rm e}(\omega) = (2/3)(e^2/m_{\rm e}c^3)\,\omega^2$. Then the terms containing factor α in equation (B3) cancel out, and it simplifies to

$$\tilde{\nu}_\alpha(\omega) = \frac{2}{3}\,\frac{e^2}{m_* c^3}\,\omega^2 + \nu_\alpha^{\rm ff}(\omega). \tag{40}$$

5 STATISTICAL EQUILIBRIUM OF PROTON LANDAU LEVELS

5.1 Two-level system

The model in which only two quantum levels participate in the radiative and collisional transitions is helpful for understanding the main features of line formation and transition rates. This simplest model can be applicable to the formation of the proton cyclotron line if the ground Landau level is much more populated than excited ones. For *electron* cyclotron lines, a similar model was considered previously by Nagel & Ventura (1983).

The statistical equilibrium of two proton Landau levels is given by the equation

$$n_0\left(\Gamma_{01}^B + \Gamma_{01}^C\right) = n_1\left(\Gamma_{10}^A + \hat{\Gamma}_{10}^B + \Gamma_{10}^C\right). \tag{41}$$

Let us first consider the case where proton–proton collisions are unimportant. Then, taking into account equation (30) and the relation $\Gamma_{01}^{C(\rm pe)} = \Gamma_{10}^{C(\rm pe)}{\rm e}^{-\beta_{\rm p}}$ (Section 3.1), equation (41) can be written in the form

$$\frac{n_1}{n_0} = {\rm e}^{-\beta_{\rm p}}\,\frac{1+\epsilon\,R/(1-{\rm e}^{-\beta_{\rm p}})}{1+R+\epsilon\,R/\left({\rm e}_{\rm p}^{\beta}-1\right)}, \quad R \equiv \Gamma_{\rm r,p}/\,\Gamma_{10}^C \tag{42}$$

where the parameter $\epsilon = 2\sum_j A_+^j J_j/B_\omega$ (at $\omega = \omega_{\rm cp}$) characterizes the ratio of the effective radiative energy density in the line to its equilibrium value.

Let us mention three important limiting cases.

(i) When either $R \ll 1$ or $\epsilon = 1$, the Boltzmann ratio $n_1/n_0 = {\rm e}^{-\beta_{\rm p}}$ is recovered. This is the LTE situation, where absorption and emission coefficients are related by the Kirchhoff law.

(ii) In another limiting case, where $R \gg 1$ and $\epsilon R \ll 1$, $n_1/n_0 = {\rm e}^{-\beta_{\rm p}}/R = \Gamma_{01}^C/\,\Gamma_{\rm r,p}$, that is, excitation of the level $N = 1$ is collisional, but its deexcitation is radiative. This is the case for which emission is most prominent.

(iii) In the third limit, where $\epsilon \ll 1$ and $\epsilon R \gg 1$, the level $N = 1$ is excited by absorption of radiation and deexcited by spontaneous emission. In this case $n_1/n_0 = (8\pi^3c^2/\hbar\omega^3)\sum_j A_+^j J_j$, and

$$n_1\sum_j\int {\rm d}\mathbf{n} A_{10}(j,\omega,\mathbf{n}) = n_0\sum_j\int {\rm d}\mathbf{n} B_{01}(j,\omega,\mathbf{n})\bar{I}_{\omega,j}.$$

Then the spectral power of spontaneous emission is identical to that of absorption, and both processes can be treated as non-coherent scattering (Ventura 1979; Mészáros 1992). Such situation is most common for the electron cyclotron absorption and emission in strong magnetic fields of neutron stars (Nagel & Ventura 1983), but it is not so usual for ion (proton) cyclotron processes.

Taking into account proton–proton collisions, from equation (41) we obtain

$$\frac{n_1}{n_0} = \frac{1}{2+2\,c_{10}^{(1)}}\Big\{\Big[\left(1+c_{10}^{(0)}-c_{01}^{(1)}-x_1\right)^2 + 4\left(1+c_{10}^{(1)}\right)\left(x_1+c_{01}^{(0)}\right)\Big]^{1/2} - \left(1+c_{10}^{(0)}-c_{01}^{(1)}-x_1\right)\Big\}, \tag{43}$$

where $c_{NN'}^{(N_2)} = \frac{1}{2}n_{\rm p}\langle v_z\sigma_{NN'}^{(N_2)}\rangle/(\Gamma_{10}^A + \Gamma_{01}^B + \Gamma_{10}^{C(\rm pe)})$, the factor $\langle v_z\sigma_{NN'}^{(N_2)}\rangle$ is given by equation (18), and x_1 is the solution (42), which is reproduced when $c_{NN'}^{(0,1)} \to 0$.

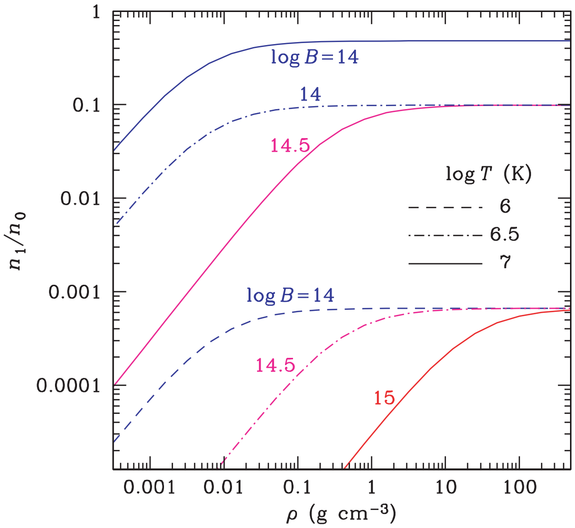

Figure 5. Population of the proton Landau level $N = 1$ relative to $N = 0$ as function of mass density for different values of B and T.

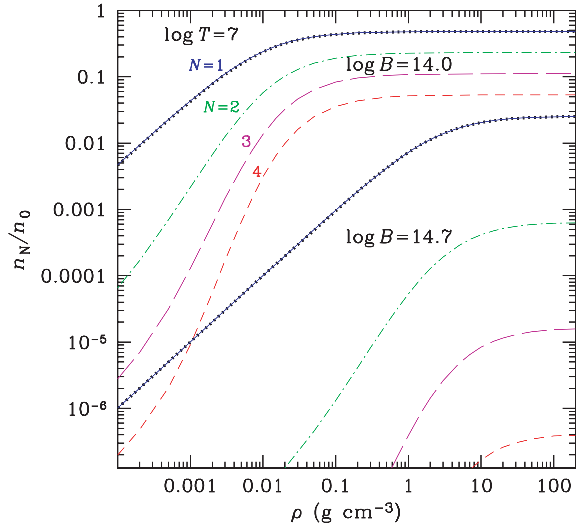

Figure 6. Populations of the levels $N = 1, 2, 3, 4$ relative to $N = 0$ as functions of mass density for $T = 10^7$ K and two values of B. The solid lines show the population of the $N = 1$ level, dot–dashed lines $N = 2$, long-dashed lines $N = 3$ and short-dashed lines $N = 4$. The dotted lines show n_1/n_0 based on the two-level approximation.

In Fig. 5 we show the relative populations of the excited proton Landau state ($N = 1$) as function of density, according to equation (43), for several B and T values. Here we assumed that stimulated transitions are unimportant and set $\epsilon = 0$ in equation (42). At high density, all curves tend to their LTE limit $n_1/n_0 = \mathrm{e}^{-\beta_\mathrm{p}}$. Radiative decay rates dominate at lower densities, where the excited level becomes depopulated.

For the considered plasma parameters, the rates of transitions due to proton–proton collisions are of the same order of magnitude or smaller than those due to electron–proton collisions. Therefore a neglect of the *pp* rates does not significantly affect the statistical equilibrium. For instance, in Fig. 5 this neglect would change n_1/n_0 by less than 6 per cent. Thus statistical equilibrium can be approximately evaluated with only proton–electron interactions taken into account.

5.2 Multilevel system

The statistical equilibrium of proton distribution over Landau levels is determined by the balance of the total rates of transitions from and to every level N,

$$n_N \left[\sum_{N'<N} \Gamma^A_{NN'} + \sum_{N'\neq N} \left(\Gamma^B_{NN'} + \Gamma^C_{NN'} \right) \right] = \sum_{N'>N} n_{N'}\, \Gamma^A_{N'N} + \sum_{N'\neq N} n_{N'} \left(\Gamma^B_{N'N} + \Gamma^C_{N'N} \right), \tag{44}$$

supplemented with the condition $\sum_N n_N = n_\mathrm{p}$. Here $\Gamma^C_{NN'} = \Gamma^{C(\mathrm{pe})}_{NN'} + \Gamma^{C(\mathrm{pp})}_{NN'}$. This system is non-linear, because according to equation (15) $\Gamma^{C(\mathrm{pp})}_{NN'}$ depends on the distribution of n_N. We solve equation (44) iteratively, starting from the Boltzmann distribution of n_N.

An example of the numerical solution of equation (44) is shown in Fig. 6. As in Fig. 5, here we have neglected Γ^B relative to Γ^C. The curves of different style correspond to the values of n_N/n_0 as functions of ρ for different N from 1 to 4. The dots correspond to n_1/n_0 in the two-level approximation (cf. Fig. 5). We see that they coincide with the multilevel solution for n_1/n_0 (solid lines) within graphical accuracy.

6 OPACITY AND EMISSIVITY

6.1 Relation between emission and absorption coefficients

For each polarization component, the photoabsorption coefficient can be presented in the form

$$\mu(\omega) = \sum_{N,N'} \mu_{NN'}(\omega), \tag{45}$$

$$\mu_{NN'}(\omega) = n_N \int \mathcal{F}_N(v_z)\, \sigma_{NN'}(v_z,\omega)\mathrm{d}v_z - n_{N'} \int \mathcal{F}_{N'}(v'_z)\, \sigma_{NN'}(v_z,\omega)\,\mathrm{d}v'_z, \tag{46}$$

where $\sigma_{NN'}(v_z,\omega)$ is the (free–free) partial photoabsorption cross-section for ions in the Landau state N having longitudinal velocity v_z and going to the final state N', and $\mathcal{F}_N(v_z)$ is the distribution of v_z for such ions.[3] The second term in equation (46) represents stimulated emission (treated as negative absorption), v'_z is related to v_z by the energy conservation law $m_\mathrm{p}v_z^2/2 + E_{N,\perp} + \hbar\omega = m_\mathrm{p}v_z'^2/2 + E_{N',\perp}$, and the integration is performed over those v_z for which this law can be satisfied. In the case where $\mathcal{F}_N(v_z) = \mathcal{F}_{m_\mathrm{p},T}(v_z)$ is the Maxwellian distribution (10) with T independent of N, equation (46) can be written as

$$\mu_{NN'}(\omega) = n_N \sigma_{NN'}(\omega) \left[1 - \frac{n_{N'}}{n_N}\, \mathrm{e}^{(N'-N)\beta_\mathrm{p} - \hbar\omega/T} \right], \tag{47}$$

where $\sigma_{NN'}(\omega) = \int \mathcal{F}_N(v_z)\,\sigma_{NN'}(v_z,\omega)\mathrm{d}v_z$. In LTE, equations (45)–(47) yield

$$\mu^\mathrm{LTE}(\omega) = n_\mathrm{p}\sigma(\omega)\,(1 - \mathrm{e}^{-\hbar\omega/T}), \tag{48}$$

where $n_\mathrm{p} \equiv \sum_N n_N$ and $\sigma(\omega)$ is the average photoabsorption cross-section of a proton: $\sigma(\omega) = \sum_N f^\mathrm{p}_N \sum_{N'} \sigma_{NN'}(\omega)$.

[3] This is essentially the partial cross-section given by equation (33), except that the latter assumes $v_z = 0$. To simplify notations, we suppress the subscript 'α' and the superscript 'ff' in this section.

The power of spontaneous emission of unit volume into d ω d **n** is j_ω d ω d **n**, where j_ω is the *emission coefficient*. Some authors (e.g. Zheleznyakov 1996) call it emissivity (whereas other authors, e.g. Rybicki & Lightman 1979 call emissivity the emission power per unit mass). It can be derived from the second Einstein relation (22) and presented in the form

$$j_\omega = \sum_{N'N} j_{\omega,N'N}, \tag{49}$$

$$j_{\omega,N'N} = \frac{\hbar\omega^3}{8\pi^3 c^2} n_{N'} \int \mathcal{F}_{N'}(v_z')\,\sigma_{NN'}(v_z,\omega)\,\mathrm{d}v_z'. \tag{50}$$

In the case of Maxwell–Boltzmann distribution of v_z and v_z', using equation (47) we obtain

$$j_{\omega,N'N} = \frac{\hbar\omega^3}{8\pi^3 c^2}\, n_{N'}\, \sigma_{NN'}(\omega)\, \mathrm{e}^{(N'-N)\beta_\mathrm{p} - \hbar\omega/T}. \tag{51}$$

In LTE, equations (45), (49) and (51) reduce to the Kirchhoff law (for each polarization mode)

$$j_\omega^\mathrm{LTE} = \mu^\mathrm{LTE}(\omega) B_\omega(T)/2. \tag{52}$$

According to equation (51), the ratio of the emission coefficient to its LTE value (often also called emissivity) is

$$\frac{j_\omega}{j_\omega^\mathrm{LTE}} = \sum_{N'N} \frac{\mu_{NN'}(\omega)}{\mu^\mathrm{LTE}(\omega)} \left(\mathrm{e}^{\hbar\,\omega/T} - 1\right) \times \left[\frac{n_N}{n_{N'}}\,\mathrm{e}^{(N-N')\beta_\mathrm{p} + \hbar\,\omega/T} - 1\right]^{-1}. \tag{53}$$

We shall call ratio (53) *relative emissivity*.

6.2 Proton cyclotron line

Figs 7 and 8 show the opacities $\mu(\omega)/\rho$ (upper panels) and relative emissivities $j_\omega/j_\omega^\mathrm{LTE}$ (lower panels) as functions of the photon energy for polarization $\alpha = +1$, for two values of ρ and two values of B. At $\omega \ll \omega_\mathrm{cp}$, the main contribution to the absorption and emission of photons is given by the free–free processes preserving N ($N = N'$). In this case $j_\omega \approx j_\omega^\mathrm{LTE}$. At higher ω, transitions $N \to N' \neq N$ give a noticeable contribution to the photoabsorption. In the absence of statistical equilibrium, they result in a decrease of the relative emissivity ($j_\omega < j_\omega^\mathrm{LTE}$).

The Coulomb logarithms for photoabsorption processes $N \to N'$ strongly increase at $\omega \approx (N' - N)\omega_\mathrm{cp}$. At these frequencies the weight of such transitions increases, which causes weak spikes (pseudoresonances) in the photoabsorption cross-sections (see Potekhin & Chabrier 2003). However, at the ρ, T, and B values shown in Figs 7 and 8, the resonant peaks of the Coulomb logarithms $\Lambda^{\mathrm{ff},+1}_{0,N;0,N'}(N' > N)$ are not sufficiently high to make them larger than $\Lambda^{\mathrm{ff},+1}_{0,N;0,N}$. Therefore the free–free absorption/emission processes with $N' = N$ give the main contribution even at $\omega \approx (N' - N)\omega_\mathrm{cp}$. Accordingly, these pseudoresonances are not very pronounced. They are not visible in the opacity curves in the upper panels of Figs 7 and 8 because of the logarithmic scale, but the corresponding periodic decreases of the relative emissivity at multiples of ω_cp are clearly seen in the lower panels.

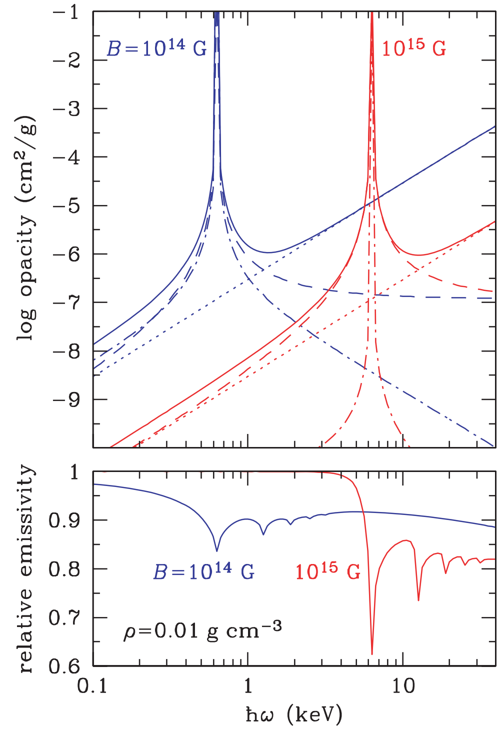

Figure 7. Upper panel: the opacity components for the polarization $\alpha = +1$, as functions of the photon energy, for $\rho = 0.01$ g cm^{-3}, $T = 10^7$ K and $B = 10^{14}$ and 10^{15} G (as marked near the curves). Dashed lines – ion scattering opacity, dotted lines – electron scattering opacity, dot–dashed lines – free–free absorption contribution, solid lines – the total. Lower panel: relative emissivity, equation (53), for the same plasma parameters.

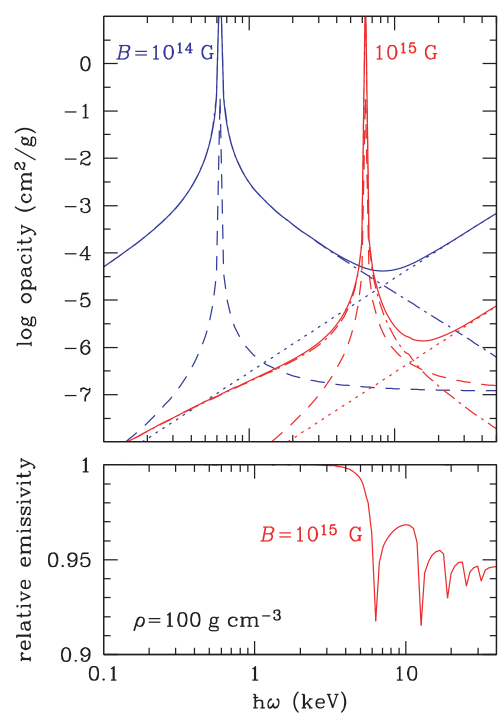

Figure 8. The same as in Fig. 7 but for $\rho = 100$ g cm^{-3}. In this case the relative emissivity for the weaker field ($B = 10^{14}$ G) equals to one because of the LTE.

7 GENERALIZATION FOR OTHER IONS

The formulae derived in the present paper for protons can be generalized for other nuclei with arbitrary A and Z. If they have spin $\frac{1}{2}$, then in the formulae for the rates of non-radiative collisions it is sufficient to replace the mass m_p by $m_i = 0.9928\,Am_p$, the number density n_p by $n_i = n_e/Z$, the magnetic field parameter β_p by $\beta_i \equiv \hbar\omega_{ci}/T = 73.9(Z/A)\,B_{14}/T_6$, and to use for the Debye screening wave number the Z-dependent formula $k_s^2 = 4\pi(1+Z)n_e e^2/T$. Furthermore, in equation (8) one should replace $I_{NN'}(t/2)$ by $I_{NN'}(t/2Z)$ and use equation (A21), $u'^2 = u^2 + 2Z(N-N')m_*/m_i$. Also in equation (16) one should substitute $w(u_\pm)$ and $w^x(u_+, u_-)$ from equations (A19) (with $Z_1 = Z_2 = Z$) and (A24), and to use $u'^2 = u^2 + Z\,(N - N' + N_2 - N'_2)$ from equation (A21).

Generalization for ions with different spin is also straightforward, but more elaborate, because it requires to rewrite equation (18) with allowance for different projections of spin on the magnetic field.

A possible generalization of the free–free cross-section $\sigma^{\rm ff}$ for $Z \neq 1$ is discussed at the end of Appendix B.

8 SUMMARY

We have derived the general expressions for the rates of transitions between ion Landau levels caused by non-radiative and radiative electron–ion Coulomb collisions and non-radiative ion-ion collisions. We have also obtained (in Appendix B) the formulae for free–free photoabsorption cross-sections in strong magnetic fields with allowance for the electron and ion (proton) quantization, which are much simpler than the previously known ones.

On the base of the calculated transition rates we solved the equation of statistical equilibrium for protons in a strong magnetic field. Considerable deviation from the Boltzmann distribution over the proton Landau levels occurs at densities $\rho \lesssim 0.1\,B_{14}^{3.5}$ g cm^{-3}. At higher densities (lower magnetic fields) non-LTE effects are negligible. Conversely, at lower densities (higher B) the excited proton states become depleted because of radiative decay.

Nevertheless, even with strongly depleted populations of the excited Landau states, the emissivity of the fully ionized plasma is not much suppressed relative to its LTE value. This is because the main contribution in the photoabsorption is given by transitions which do not change Landau number N. For such transitions, the relative population of other levels is unimportant.

Although we have performed calculations only for the proton–electron plasma, generalization of our results to other ions is rather straightforward (Section 7).

All results in the present paper are obtained in the Born approximation. A truncation used in older papers to eliminate the divergence at small velocities, inherent to the Born approximation, is now replaced by a smooth correction. The thermally averaged electron–proton non-radiative and radiative transition rates are not sensitive to this correction. Proton–proton transition rates, however, are sensitive, therefore their more thorough examination beyond the Born approximation would be desirable. Fortunately, at the considered physical conditions the proton–proton rates are not dominant, thus we think that our main conclusions are sufficiently robust.

Our general expressions for the proton/ion Landau level transitions derived in this paper will be useful for studying the possibility and the conditions of proton/ion cyclotron line formation in magnetar bursts. The radiation-dominated bubble formed during the magnetar outbursts may be considered as a hot ($T \gtrsim 10$ keV), optically thick, rarefied medium embedded in a strong magnetic field (Thompson & Duncan 1995; Woods & Thompson 2005). Within the bubble, vacuum polarization dominates the dielectric tensor and scattering dominates the opacity. The bubble may also contains appreciable amount of ions ripped out of the NS surface during the outbursts. A neutron star atmosphere code, such as that developed in Ho & Lai (2001, 2003) and van Adelsberg & Lai (2006), can be adapted to study radiative transfer in the bubble. It may be that depending on the total bubble energy and the location of energy release in the bubble, the characteristics of bubble radiation (such as ion cyclotron line strength, line emission vs. absorption) are different. If so, the burst spectra can provide a useful diagnostics for the energy dissipation mechanisms of magnetar outbursts.

ACKNOWLEDGMENTS

A.P. thanks Gérard Massacrier for enlightening discussions of quantum effects on spectral line formation, and theoretical astrophysics groups of the Astronomy Department of Cornell University and of the Ecole Normale Supérieure de Lyon for hospitality. This work has been supported in part by NSF grant AST 0307252, and *Chandra* grant TM6-7004X (Smithsonian Astrophysical Observatory). The work of A.P. is supported in part by FASI grant NSh-9879.2006.2 and RFBR grants 05-02-16245 and 05-02-22003.

REFERENCES

Araya R. A., Harding A. K., 1999, ApJ, 517, 334
Araya-Góchez R. A., Harding A. K., 2000, ApJ, 544, 1067
Baring M. G., Gonthier P. L., Harding A. K., 2005, ApJ, 630, 430
Burnard D. J., Klein R. I., Arons J., 1988, ApJ, 324, 1001
Canuto V., Lodenquai J., Ruderman M., 1971, Phys. Rev. D, 3, 2303
Cohen-Tannoudji C., Dupont-Roc J., Grynberg G., 1998, Atom–Photon Interactions: Basic Processes and Applications. Wiley-VCH, Berlin
Daugherty J. K., Ventura J., 1977, A&A, 61, 723
Daugherty J. K., Ventura J., 1978, Phys. Rev. D, 18, 1053
Gavriil F. P., Kaspi V. M., Woods P. M., 2002, Nat, 419, 142
Ginzburg V. L., 1970, The Propagation of Electromagnetic Waves in Plasmas, 2nd edn. Pergamon, London
Haberl F. et al., 2004, A&A, 424, 635
Hasegawa H., Howard R. E., 1961, J. Phys. Chem. Solids, 21, 179
Heindl W. A., Rothschild R. E., Coburn W., Staubert R., Wilms J., Kreykenbohm I., Kretschmar P., 2004, in Kaaret P., Lamb F. K., Swank J. H., eds, AIP Conf. Proc. Vol. 714, X-ray Timing 2003: Rossi and Beyond. Am. Inst. Phys., Melville, NY, p. 323
Ho W. C. G., Lai D., 2001, MNRAS, 327, 1081
Ho W. C. G., Lai D., 2003, MNRAS, 338, 233
Ho W. C. G., Lai D., 2004, ApJ, 607, 420
Ibrahim A. L., Swank J. H., Parke W., 2003, ApJ, 584, L17
Jackson J. D., 1975, Classical Electrodynamics, 2nd edn. Wiley, New York
Juett A. M., Marshall H. L., Chakrabarty D., Schulz N. S., 2002, ApJ, 568, L31
Kaminker A. D., Yakovlev D. G., 1981, Theor. Math. Phys., 49, 1012
Klepikov N. P., 1954, Zh. Eksp. Teor. Fiz., 26, 19 (in Russian)
Kulkarni S. R., Kaplan D. L., Marshall H. L., Frail D. A., Murakami T., Yonetoku D., 2003, ApJ, 585, 948
Lai D., Ho W. C. G., 2003, ApJ, 588, 962
Lamb D. Q., Masters A. R., 1979, ApJ, 234, L117
Lamb D. Q., Wang J. C. L., Wasserman I., 1990, ApJ, 363, 670
Landau L. D., Lifshitz E. M., 1976, Quantum Mechanics. Pergamon, Oxford
Langer S. H., 1981, Phys. Rev. D, 23, 328 (erratum: 1982, Phys. Rev. D, 25, 1157)
McLaughlin M. A. et al., 2003, ApJ, 591, L135
Melrose D. B., Zheleznyakov V. V., 1981, A&A, 95, 86
Mészáros P., 1992, High-Energy Radiation from Magnetized Neutron Stars. Univ. Chicago Press, Chicago
Mészáros P., Nagel W., 1985, ApJ, 299, 138
Miller G. S., Salpeter E. E., Wasserman I., 1987, ApJ, 314, 215
Nagel W., Ventura J., 1983, A&A, 118, 66
Patel S. K. et al., 2003, ApJ, 587, 367
Pavlov G. G., Panov A. N., 1976, Sov. Phys. – JETP, 44, 300
Pavlov G. G., Yakovlev D. G., 1976, Sov. Phys. – JETP, 43, 389

Pavlov G. G., Bezchastnov V. G., Mészáros P., Alexander S. G., 1991, ApJ, 380, 541
Pavlov G. G., Shibanov Yu. A., Zavlin V. E., Meyer R. D., 1995, in Alpar M. A., Kiziloğlu Ü.,van Paradijs J., eds, NATO ASI Ser. C, Vol. 450, The Lives of the Neutron Stars. Kluwer, Dordrecht, p. 71
Potekhin A. Y., 1996, A&A, 306, 999
Potekhin A. Y., Chabrier G., 2003, ApJ, 585, 955
Potekhin A. Y., Pavlov G. G., 1997, ApJ, 483, 414
Potekhin A. Y., Pavlov G. G., Ventura J., 1997, A&A, 317, 618
Potekhin A. Y., Lai D., Chabrier G., Ho W. C. G., 2004, ApJ, 612, 1034
Potekhin A. Y., Lai D., Chabrier G., Ho W. C. G., 2005, Adv. Space Res., 35, 1158
Rea N., Israel G. L., Stella L., Oosterbroek T., Mereghetti S., Angelini L., Campana S., Covino S., 2003, ApJ, 586, L65
Rea N., Oosterbroek T., Zane S., Turolla R., Méndez M., Israel G. L., Stella L., Haberl F., 2005, MNRAS, 361, 710
Rybicki G. B., Lightman A. P., 1979, Radiative Processes in Astrophysics. Wiley, New York
Sokolov A. A., Ternov I. M., 1986, Radiation from Relativistic Electrons, 2nd edn. Am. Inst. Phys., New York
Storey M. C., Melrose D. B., 1987, Aust. J. Phys., 40, 89
Strohmayer T. E., Ibrahim A. I., 2000, ApJ, 537, L111
Terada Y. et al., 2006, ApJ, 648, L139
Thompson C., Duncan R. C., 1995, MNRAS, 275, 255
Thompson C., Duncan R. C., 1996, ApJ, 473, 322
Tiengo A., Mereghetti S., Turolla R., Zane S., Rea N., Stella L., Israel G. L., 2005, A&A, 437, 997
Trümper J., Pietsch W., Reppin C., Voges W., Staubert R., Kendziorra E., 1978, ApJ, 219, L105
van Adelsberg M., Lai D., 2006, MNRAS, 373, 1495
van Kerkwijk M. H., Kaplan D. L., 2006, Ap& SS, in press (astro-ph/0607320)
van Kerkwijk M. H., Kaplan D. L., Durant M., Kulkarni S. R., Paerels F., 2004, ApJ, 608, 432
Ventura J., 1973, Phys. Rev. A, 8, 3021
Ventura J., 1979, Phys. Rev. D, 19, 1684
Ventura J., Nagel W., Mészáros P., 1979, ApJ, 233, L125
Wang J. C. L., Wasserman I., Lamb D. Q., 1993, ApJ, 414, 815
Wasserman I., Salpeter E. E., 1980, ApJ, 241, 1107
Woods P. M., Thompson C., 2005, in Lewin W. H. G., van der Klis M., eds, Compact Stellar X-Ray Sources. Cambridge Univ. Press, Cambridge
Zane S., Turolla R., Stella L., Treves A., 2001, ApJ, 560, 384
Zheleznyakov V. V., 1996, Radiation in Astrophysical Plasmas. Kluwer, Dordrecht

APPENDIX A: TRANSITION RATES FOR COULOMB SCATTERING

Here we present the non-relativistic formulae for the collision rates of charged particles in an arbitrary magnetic field, derived in the Born approximation.

A1 Scattering off a fixed Coulomb centre

A1.1 Derivation of the cross-section for $Z = 1$

The motion of a charged particle in a magnetic field can be described by different sets of wave functions, corresponding to different choices of the electromagnetic gauge (e.g. Landau & Lifshitz 1976). Ventura (1973) studied the scattering by a fixed Coulomb potential using the axially symmetric gauge of the vector potential $\boldsymbol{A} = \frac{1}{2}\boldsymbol{B} \times \boldsymbol{r}$. Pavlov & Yakovlev (1976) found that the Landau gauge $(A_x, A_y, A_z) = (0, -By, 0)$ facilitates obtaining a simpler representation of the scattering rate. In the latter gauge, the 'good' quantum numbers are the Landau number N and the components k_x and k_z of the wave vector of the particle. Assuming $Z = 1$, one can write the coordinate wave function as

$$\psi_{N,k_x,k_z}(\boldsymbol{r}) = (L_x L_z)^{-1/2} \mathrm{e}^{\mathrm{i}k_x x + \mathrm{i}k_z z} \chi_N\left(y + k_x a_\mathrm{m}^2\right), \tag{A1}$$

where

$$\chi_N(y) = \frac{\exp\left(-y^2/2a_\mathrm{m}^2\right)}{\pi^{1/4}(2^N N!\, a_\mathrm{m})^{1/2}} H_N(y/a_\mathrm{m}), \tag{A2}$$

and $H_N(\xi) = (-1)^N \mathrm{e}^{\xi^2} \mathrm{d}^N \mathrm{e}^{-\xi^2}/\mathrm{d}\xi^N$ is a Hermite polynomial. The functions $\chi_N(y)$ are ortho-normalized and have the following nice property (Klepikov 1954; Kaminker & Yakovlev 1981):

$$\int_{-\infty}^{\infty} \chi_N\left(y - q_x a_\mathrm{m}^2/2\right) \chi_{N'}\left(y + q_x a_\mathrm{m}^2/2\right) \mathrm{e}^{\mathrm{i}q_y y} \mathrm{d}y = I_{N'N}\left(q_\perp^2 a_\mathrm{m}^2/2\right) \mathrm{e}^{\mathrm{i}(N'-N)\arctan(q_y/q_x)}. \tag{A3}$$

Here $q_\perp^2 \equiv q_x^2 + q_y^2$, and $I_{N'N}$ is the Laguerre function (Sokolov & Ternov 1986), defined as follows: if $N' - N \geqslant 0$, then

$$I_{N'N}(x) = \sqrt{\frac{N!}{N'!}}\, \mathrm{e}^{-x/2} x^{(N'-N)/2} L_N^{N'-N}(x) = \mathrm{e}^{-x/2} x^{(N'-N)/2} \sum_{l=0}^{N} \frac{\sqrt{N!N'!}\,(-x)^l}{l!\,(N-l)!\,(N'-N+l)!}, \tag{A4}$$

otherwise $I_{N'N}(x) = (-1)^{N-N'} I_{NN'}(x)$; $L_N^s(x)$ is generalized Laguerre polynomial.

Relation (A3) allows one to reduce the matrix element of the transition $|Nk_x k_z\rangle \to |N'k_x' k_z'\rangle$ to the form

$$M = \frac{1}{2\pi L_x L_z} \int_{-\infty}^{\infty} \mathrm{e}^{-\mathrm{I}q_y(k_x+k_x')a_\mathrm{m}^2/2 + \mathrm{i}(N'-N)\arctan(q_y/q_x)} \times I_{N'N}\left(q_\perp^2 a_\mathrm{m}^2/2\right) V_q\, \mathrm{d}q_y, \tag{A5}$$

where $q_x = k'_x - k_x$, $q_z = k_z' - k_z$, and

$$V_q = e^2 \int \mathrm{d}\boldsymbol{r}\, \mathrm{e}^{\mathrm{i}\boldsymbol{q}\cdot\boldsymbol{r}} \frac{e^{-k_\mathrm{s} r}}{r} = \frac{4\pi e^2}{q^2 + k_\mathrm{s}^2} \tag{A6}$$

is the Fourier transform of the potential. In this paper we use the screened Coulomb potential for the electron–ion non-degenerate plasma, for which k_s equals the inverse Debye screening length.

Averaging the specific transition rate $(2\pi/\hbar)|M|^2\ \delta(E' - E)$ (where E and E' is the initial and final energy) over k_x and summing it over k_x' and k_z' we obtain the transition rate per particle on the level N with initial longitudinal velocity $v_z = \hbar k_z/m$, in a volume $V = L_x L_y L_z$:

$$W_{NN'}^\mathrm{fix} \equiv \frac{v_z \sigma_{NN'}^\mathrm{fix}(v_z)}{V} = \frac{L_x L_z}{(2\pi)^2} \frac{a_\mathrm{m}^2}{L_y} \sum_\pm \int_{-\infty}^{\infty} \mathrm{d}k_x \int_{-\infty}^{\infty} \mathrm{d}k_x' \frac{2\pi}{\hbar} |M|^2 \left(\frac{\mathrm{d}E'}{\mathrm{d}|k_z'|}\right)^{-1} = \frac{4\pi}{\tau_0} \frac{m}{m_\mathrm{e}} \frac{a_\mathrm{m}^3}{V} \sum_\pm \frac{w_{NN'}^\mathrm{fix}(u_\pm)}{u'}, \tag{A7}$$

where $\tau_0 = \hbar^3/e^4 m_\mathrm{e}$ is the atomic unit of time, $\sigma_{NN'}^\mathrm{fix}(v_z)$ is an effective partial cross-section,

$$w_{NN'}^\mathrm{fix}(u_\pm) = \int_0^\infty \frac{I_{N'N}^2(t/2)}{(t + u_\pm^2)^2}\, \mathrm{d}t, \tag{A8a}$$

$$u_\pm = \left[(u \pm u')^2 + u_\mathrm{s}^2\right]^{1/2}, \quad u = |k_z| a_\mathrm{m}, \quad u_\mathrm{s} = k_\mathrm{s} a_\mathrm{m}, \tag{A8b}$$

$$u' = |k_z'| a_\mathrm{m} = \sqrt{u^2 + 2N - 2N'}, \tag{A8c}$$

and $w^{\rm fix}_{NN'}$ should be set equal to zero when $u^2 < 2(N' - N)$. It is easy to check that equations (A7), (A7) are equivalent to equations (12), (13) of Pavlov & Yakovlev (1976).

A1.2 Classical limit

The function $w^{\rm fix}_{NN'}(u_\pm)$ belongs to a class of integrals studied by Potekhin (1996). According to his equation (B21), based on Kaminker & Yakovlev (1981), in the semiclassical limit

$$w^{\rm fix}_{NN'}(u_\pm) \approx (1/2)\left(u_\pm^2/2 + N + N'\right) \times \left[(\sqrt{N'} - \sqrt{N})^2 + u_\pm^2/2\right]^{-3/2} \times \left[(\sqrt{N'} + \sqrt{N})^2 + u_\pm^2/2\right]^{-3/2} \quad (N \gg 1,\ N' \gg 1). \tag{A9}$$

Using this approximation, one can demonstrate that equations (A7), (A7) provide the correct classical cross-section in the limit $B \to 0$, where N can be replaced by $(p_\perp a_{\rm m}/\hbar)^2/2$, $\boldsymbol{p} = m\boldsymbol{v} = \hbar\boldsymbol{k}$, $p_\perp^2 \equiv p_x^2 + p_y^2$. For example, consider a scattering event without screening ($k_{\rm s} = 0$), where the particle moves in the xz plane at the angle θ to the z axis before scattering and $\theta' = \theta + \alpha$ after scattering, $\theta < \pi/2$, and $\theta' < \pi/2$. Taking into account that $p' = p$ and $(p_z' p_z - p_\perp' p_\perp)/p^2 = \cos\alpha = 1 - 2\sin^2\alpha/2$, from equation (A9) we obtain

$$w^{\rm fix}_{NN'}(u_-) = \left(\frac{\hbar}{a_{\rm m}}\right)^4 \frac{1}{8p^3\,\sin^4\alpha/2}\,\frac{1 - \cos\theta\cos\theta'}{1 - \cos\alpha}. \tag{A10}$$

When $N' \gg 1$, a sum over N' can be replaced by an integral. Then, according to equations (A7) and (A10), the effective cross-section for transitions into a range of Landau levels between N' and $N' + {\rm d}N'$ is

$$\begin{aligned}{\rm d}\sigma &= \frac{4\pi}{\tau_0}\,\frac{m}{m_{\rm e}}\,\frac{a_{\rm m}^3}{v_z}\,\frac{w(u_-)}{u'}\,{\rm d}N' = \frac{4\pi}{\tau_0}\,\frac{m}{m_{\rm e}}\,\frac{a_{\rm m}^4}{V\hbar}\,w(u_-)\,\frac{p_\perp'\,{\rm d}p_\perp'}{p_z'}\\ &= \frac{\pi e^4 m\,(1 - \cos\theta\cos\theta')\sin\theta'}{2Vp^3\,(1 - \cos\alpha)\,\sin^4\alpha/2}\,{\rm d}\theta'.\end{aligned} \tag{A11}$$

In the cylindrically symmetric case, when $\theta \to 0$ and $\theta' \to \alpha$, equation (A11) becomes

$${\rm d}\sigma = \frac{e^4}{4m^2 v_z^4}\,\frac{1}{\sin^4\alpha/2}\,{\rm d}\Omega_\alpha, \tag{A12}$$

where ${\rm d}\Omega_\alpha$ is a solid angle element. This is the Rutherford formula.

A1.3 Cross-section and average transition rate for arbitrary Z

For arbitrary charges of the scattered particle, Ze, and the Coulomb centre, $Z_0 e$, one should replace $a_{\rm m} \to a_{\rm m}\,|Z|^{-1/2}$ in equations (A1)–(A5) and $V_q \to Z_0 Z V_q$ in equation (A5). Then

$$\sigma^{\rm fix}_{NN'}(v_z) = \frac{4\pi a_{\rm m}^3}{v_z \tau_0}\,\frac{m}{m_{\rm e}}\,Z_0^2\sqrt{|Z|}\sum_\pm \frac{w^{\rm fix}_{NN'}(u_\pm)}{u'}, \tag{A13}$$

where $w^{\rm fix}_{NN'}$, $u_\pm$, and u' are given by equations (A7) with modified scaling of k_z and k_z', $u = |k_z| a_{\rm m} |Z|^{-1/2}$ and $u' = |k_z'| a_{\rm m}\,|Z|^{-1/2}$. Besides, the Z-dependence of the Debye screening parameter $u_{\rm s} = k_{\rm s}\,a_{\rm m}$ should be taken into account.

If the velocities $v_z = \hbar k_z/m_{\rm i}$ have Maxwellian distribution (10), then from equation (A13) we obtain the probability for one particle in the state N in unit volume to make a transition to the state N'

$$\langle v_z \sigma^{\rm fix}_{NN'}(v_z)\rangle = \frac{4\sqrt{2\pi}}{\tau_0}\,\frac{m}{m_{\rm e}}\,Z_0^2\sqrt{|Z|}\,a_{\rm m}^3\,\tilde\Lambda^{\rm fix}_{NN'}, \tag{A14}$$

where $\tilde\Lambda^{\rm fix}_{NN'} \equiv \sqrt{\beta}\,\Lambda^{\rm fix}_{NN'}$,

$$\Lambda^{\rm fix}_{NN'} = \int_0^\infty \frac{{\rm d}u}{u'}\,{\rm e}^{-\beta u^2/2}\,\theta(u'^2)\sum_\pm w^{\rm fix}_{NN'}(u_\pm), \tag{A15}$$

$\beta = \hbar|Z|eB/mcT$. The function $\theta(u'^2)$ is the step function, equal to 1 when $u^2 + 2(N - N') > 0$ and 0 otherwise.

A1.4 Validity range and correction

The integral in equation (A15) diverges when $N = N'$. This behaviour, which is well known for collision rates in the Born approximation in one dimension, means nothing but violation of this approximation for low velocities of the colliding particles.

A convenient parameter of the magnetic field strength at atomic scales is $\gamma_B = b/(\alpha_{\rm f} Z Z_0)^2 = \hbar^3 B/(m^2 c\,|Z| Z_0^2 e^3)$, where $\alpha_{\rm f}$ is the fine-structure constant. Born approximation is valid at $|k_z|$, $|k_z'| \gg |ZZ_0| e^2 m/\hbar^2$, that is at u, $u' \gg \gamma_B^{-1/2}$. The most important effect of going beyond Born approximation is the suppression of the amplitude of the longitudinal part of the wave function (the exponential in equation [A1]) near the Coulomb centre. At $|k_z| \to 0$ this amplitude becomes proportional to $\sqrt{|k_z|}$. Quantitatively, when $\ln\gamma_B \gg 1$, the ratio of the square modulus of the amplitude at $|k_z z|\,\gamma_B^{-1/4} \ll u \ll 1$ relative to its constant value at $u \gg 1$ equals $C|k_z|\hbar^2/(m|ZZ_0|e^2) = Cu\sqrt{\gamma_B}$, where $C = 2\pi/\ln^2\gamma_B\,[1 + O(1/\ln\gamma_B)]$ (Hasegawa & Howard 1961). Therefore, at $u \to 0$ or $u' \to 0$, $|M|^2$ in equation (A7) becomes proportional to u or u', respectively, which compensates the diverging factor $1/u'$ in equation (A15).

In order to eliminate the divergence of collision integrals in Born approximation, similar to equation (A15), previous authors (Pavlov & Panov 1976; Kaminker & Yakovlev 1981) introduced a cutoff at the lower limit of integration for $N = N'$. Instead of the cutoff, we introduce weight function $g(u)g(u')$, with

$$g(u) = \left(1 + \gamma_B^{-1} u^{-2}\right)^{-1/2}. \tag{A16}$$

Under the conditions $\gamma_B \gg 1$ and $\beta\gamma_B \gg 1$, Born approximation is valid for most of the velocity values that substantially contribute to the integral in equation (A15). The latter condition can be written as $T \gg Z_0^2 Z^2 e^4 m_*/\hbar^2$, which is the usual condition of the applicability of Born approximation in the non-magnetic case.

Apart from Born approximation, which consists in neglecting the influence of the Coulomb potential on the *longitudinal* part of the wave function (the exponential in equation [A1]), we have also employed the adiabatic approximation, which consists in neglecting perturbation of the *transverse* part of the wave function (χ_N in equation [A1]). For the continuum wave functions, both approximations are always valid at $z \to \infty$, but may become inaccurate at the distances from the Coulomb centre comparable to the Bohr radius. The adiabatic approximation remains sufficiently accurate at small z provided that the parameter γ_B, introduced above, is large. Lowest-order perturbation corrections and exact solution to the continuum wave functions in a strong magnetic field beyond the adiabatic approximation have been discussed, e.g. by Potekhin, Pavlov & Ventura (1997).

A2 Scattering of two charged particles

A2.1 Scattering of different particles

Let us consider Coulomb scattering of two particles with charges $Z_i e$ $(i = 1, 2)$. In the Landau gauge (Section A1) their wave functions are

$$\psi_{N_i,k_{x,i},k_{z,i}}(\boldsymbol{r}_i) = (L_x L_z)^{-1/2} \mathrm{e}^{\mathrm{i}k_{x,i}x_i + \mathrm{i}k_{z,i}z_i} \times |Z_i|^{1/4}\, \chi_N\left(|Z_i|^{1/2}\left(y_i + k_{x,i}a_{\rm m}^2/Z_i\right)\right), \quad \text{(A17)}$$

where $\chi_N(y)$ is given by equation (A2). The excitation energy of the two particles is $E = \hbar eBc^{-1}(|Z_1|/m_1 + |Z_2|/m_2) + m_1 v_{z,1}^2/2 + m_2 v_{z,2}^2/2$, where $m_{\rm i}$ are masses of the particles, and $v_{z,i}$ their longitudinal velocities.

Consider a transition in which the quantum numbers of the particles change from $N_i, k_{x,i}, k_{z,i}$ to $N'_i, k'_{x,i}, k'_{z,i} (i = 1, 2)$. Wave functions (A17) depend on x and z only through the plane-wave exponential factor, which results in conservation of the x and z components of the total momentum in the matrix element of any potential which depends only on the relative position $\boldsymbol{r}_2 - \boldsymbol{r}_1$ of the two particles: $k_{x1} + k_{x2} = k'_{x1} + k'_{x2}$, $k_{z1} + k_{z2} = k'_{z1} + k'_{z2}$. Since χ_N does not depend on $k_{z,i}$, we may choose the reference frame comoving with the centre of mass in the z direction, so that $k_{z2} = -k_{z1} \equiv k_z$. The number of final states in $\mathrm{d}k'_{x,1}\,\mathrm{d}k'_{x,2}\,\mathrm{d}k'_z$ is $(2\pi)^{-3}L_x^2 L_z\, \mathrm{d}k'_{x,1}\,\mathrm{d}k'_{x,2}\,\mathrm{d}k'_z = (2\pi)^{-3}L_x^2 L_z\,\mathrm{d}k'_{x,1}\,\mathrm{d}k'{}_{x,2}\,\mathrm{d}E'\, m_*/\hbar^2|k'_z|$, where $m_* = m_1 m_2/(m_1 + m_2)$ is the reduced mass.

Using Fourier decomposition of the interaction potential $V(\boldsymbol{r}) = (2\pi)^{-3}\int \mathrm{d}\boldsymbol{q}\, \mathrm{e}^{-\mathrm{i}\boldsymbol{q}\cdot\boldsymbol{r}}\, V_q$ (where $\boldsymbol{r} = \boldsymbol{r}_2 - \boldsymbol{r}_1$), and assuming L_x and L_z to be large, we can perform the integration over x_1, q_x, z, and q_z in the matrix element M for the transition $|N_1, N_2, k_{x,1}, k_{x,2}, k_z\rangle \to |N'_1, N'_2, k'_{x,1}, k'_{x,2}, k'_z\rangle$. This integration fixes $q_x = k_{1,x} - k'_{1,x}$ and $q_z = k'_z - k_z$ in V_q. Furthermore, using equation (A3), we can perform integration over y_1 and y_2. Then we obtain

$$M = \frac{1}{2\pi L_x^2 L_z}\int \mathrm{d}x_2\, \mathrm{e}^{\mathrm{i}(q_x + k_{x,2} - k'_{x,2})x_2} \int \mathrm{d}q_y\, V_q \times I_{N'_1 N_1}\left(\frac{q_\perp^2 a_{\rm m}^2}{2\,|Z_1|}\right) I_{N'_2 N_2}\left(\frac{q_\perp^2 a_{\rm m}^2}{2\,|Z_2|}\right) \times \exp\left[\mathrm{i}a_{\rm m}^2\left(\frac{k_{x,1}+k'_{x,1}}{2\,Z_1} - \frac{k_{x,2}+k'_{x,2}}{2\,Z_2}\right) q_y\right] \times \mathrm{e}^{\mathrm{i}\,[(N'_1 - N_1)\,\mathrm{sign}Z_1 + (N'_2 - N_2)\,\mathrm{sign}Z_2]\arctan(q_y/q_x)}. \quad \text{(A18)}$$

By averaging $|M|^2$ over $k_{x,2}$ and summing over $k'_{x,2}$, we arrive at

$$\langle |M|^2\rangle_2 \equiv \int \frac{a_{\rm m}^2\,\mathrm{d}k_{x,2}}{|Z_2|\,L_y}\int \frac{L_x\,\mathrm{d}k'_{x,2}}{2\pi}\,|M|^2 = \frac{1}{2\pi L_x^2\, L_y\, L_z^2}\int \mathrm{d}q_y\,|V_q|^2 I_{N'_1 N_1}^2\left(\frac{q_\perp^2 a_{\rm m}^2}{2\,|Z_1|}\right) I_{N'_2 N_2}^2\left(\frac{q_\perp^2 a_{\rm m}^2}{2\,|Z_2|}\right).$$

This expression does not depend on $k_{x,1}$, and therefore it does not require another averaging. Finally, summation of the specific transition rate $(2\pi/\hbar)\langle\, |M|^2\rangle_2\, \delta(E' - E)$ over $k'_{x,1}$ and k'_z gives the partial transition rate from N_1, N_2 to N'_1, N'_2 for two particles in volume $V = L_x L_y L_z$

$$W_{N_1 N_2;N'_1 N'_2} \equiv V^{-1} v_z\, \sigma_{N_1 N_2;N'_1 N'_2}(v_z) = \frac{L_z m_*}{\hbar^3 |k'_z|}\sum_{\mathrm{sign}\,k'_z}\int \frac{L_x\,\mathrm{d}k'_x}{2\pi}\,\langle |M|^2\rangle_2 = \frac{4\pi}{\tau_0}\,\frac{m_*}{m_e}\,Z_1^2 Z_2^2\,\frac{a_{\rm m}^3}{V}\,\frac{1}{u'}\sum_{\pm} w_{N_1,N_2;N'_1,N'_2}(u_\pm), \quad \text{(A19)}$$

where

$$w_{N_1,N_2;N'_1,N'_2}(u) = \int_0^\infty \frac{\mathrm{d}t}{(t+u^2)^2} \times I_{N'_1 N_1}^2\left(\frac{t}{2\,|Z_1|}\right) I_{N'_2 N_2}^2\left(\frac{t}{2\,|Z_2|}\right). \quad \text{(A20)}$$

Here $u_\pm = [(u \pm u')^2 + u_{\rm s}^2]^{1/2}$, $u = |k_z| a_{\rm m}$, $u_{\rm s} = k_{\rm s}\, a_{\rm m}$, and

$$u' = \left[u^2 + \frac{2\,m_2|Z_1|}{m_1+m_2}\,(N_1 - N'_1) + \frac{2\,m_1|Z_2|}{m_1+m_2}\,(N_2 - N'_2)\right]^{1/2}. \quad \text{(A21)}$$

The last equation represents the energy conservation law. The transition is energetically forbidden when the expression in square brackets is negative. Note that we have redefined u and u' compared to the definition used in equations (A13)–(A15): now Z_i enter equation (A21). Clearly, $w_{N_1,N_2;N'_1,N'_2}(u) = w_{N'_1,N_2;N_1,N'_2}(u) = w_{N_1,N'_2;N'_1,N_2}(u)$. In addition, if $Z_1 = Z_2$, then $w_{N_1,N_2;N'_1,N'_2}(u) = w_{N_2,N_1;N'_2,N'_1}(u)$.

A2.2 Scattering of identical particles

The derivation of the transition rates for identical particles can be patterned after Section A2.1, but with initial and final wave functions in the form $[\psi_{N_1,k_{x1},k_{z1}}(\boldsymbol{r}_1)\psi_{N_2,k_{x2},k_{z2}}(\boldsymbol{r}_2) \pm \psi_{N_1,k_{x1},k_{z1}}(\boldsymbol{r}_2)\psi_{N_2,k_{x2},k_{z2}}(\boldsymbol{r}_1)]/\sqrt{2}$, where $\psi_{N,k_x,k_z}(\boldsymbol{r})$ is given by equation (A17). The resulting partial transition rate from N_1, N_2 to N'_1, N'_2, averaged over initial and integrated over final k_x values, is

$$W^{\pm}_{N_1,N_2;N'_1,N'_2} = 2\left(W_{N_1,N_2;N'_1,N'_2} \pm W^x_{N_1,N_2;N'_1,N'_2}\right), \quad \text{(A22)}$$

where the sign + (−) refers to the states with even (odd) total spin, $W_{N_1,N_2;N'_1,N'_2}$ is given by equation (A19),

$$W^x_{N_1,N_2;N'_1,N'_2} = \frac{8\pi}{\tau_0}\,\frac{m_*}{m_e}\,\frac{|Z|^3}{u'}\,w^x_{N_1,N_2;N'_1,N'_2}(u_-, u_+), \quad \text{(A23)}$$

and

$$w^x_{N_1,N_2;N'_1,N'_2}(u_-, u_+) = \int_0^\infty \frac{\mathrm{d}t}{(t + u_+^2/|Z|)(t + u_-^2/|Z|)} \times I_{N'_1 N_1}(t/2)\, I_{N'_2 N_2}(t/2)\, I_{N'_2 N_1}(t/2)\, I_{N'_1 N_2}(t/2). \quad \text{(A24)}$$

The latter function satisfies symmetry relations $w^x_{N_1,N_2;N'_1,N'_2}(u_-, u_+) = w^x_{N_1,N_2;N'_1,N'_2}(u_+, u_-) = w^x_{N_2,N_1;N'_1,N'_2}(u_-, u_+) = w^x_{N_1,N_2;N'_2,N'_1}(u_-, u_+) = w^x_{N'_1,N'_2;N_1,N_2}(u_-, u_+)$.

APPENDIX B: CROSS-SECTIONS OF FREE–FREE PHOTOABSORPTION

In order to calculate a cross-section of the free–free absorption in a magnetic field, it is important to take into account the the ion–electron centre of mass motion effects, even though $m_p \gg m_e$. Potekhin & Chabrier (2003) performed quantum calculations of this cross-section and demonstrated a correspondence to the classical dielectric tensor (Ginzburg 1970). The result can be written as

$$\sigma_\alpha^{\rm ff}(\omega) = \frac{4\pi e^2}{m_e c}\,\frac{\omega^2\,\nu_\alpha^{\rm ff}(\omega)}{(\omega + \alpha\omega_{\rm ce})^2(\omega - \alpha\omega_{\rm cp})^2 + \omega^2\tilde{\nu}_\alpha^2(\omega)}, \quad \text{(B1)}$$

$$\nu_\alpha^{\rm ff}(\omega) = \sum_{n,N} f_n^e f_N^{\rm p} \sum_{n',N'} \nu_{n,N;n',N'}^{\rm ff,\alpha}(\omega), \tag{B2}$$

$$\tilde\nu_\alpha(\omega) = \left(1+\alpha\,\frac{\omega_{\rm ce}}{\omega}\right)\nu_p(\omega) + \left(1-\alpha\,\frac{\omega_{\rm cp}}{\omega}\right)\nu_e(\omega) + \nu_\alpha^{\rm ff}(\omega). \tag{B3}$$

Here $\alpha = 0, \pm 1$ is the polarization index, $\nu_\alpha^{\rm ff}$ is the effective frequency of the electron–ion collisions for a given photon frequency ω, $f_N^{\rm p}$ and $f_n^{\rm e}$ are the fractions of the protons and electrons in Landau states N and n, $\sigma^{\rm ff}_{\alpha;n,N;n',N'}(\omega)$ is a partial photoabsorption cross-section for a transition in which the electron and proton change their Landau quantum numbers from n to n' and from N to n', respectively. Finally, ν_p and ν_e in equation (B3) are effective damping factors for protons and electrons, respectively, not related to the electron–proton collisions (for example, Ginzburg 1970 considers collisions of electrons and protons with molecules). The derivation of the damping factor (B3) from the complex dielectric tensor of the plasma assumes $\nu_e \ll \omega_{\rm ce}$, $\tilde\nu_\alpha \ll \omega_{\rm ce}$, and $\nu_p \ll \omega_{\rm cp}$.

Potekhin & Chabrier (2003) calculated $\nu^{\rm ff,\alpha}_{n,N;n',N'}(\omega)$ assuming LTE. Following their approach without LTE, however retaining the Maxwell longitudinal distributions (10), we present the result as follows:

$$\nu^{\rm ff,\alpha}_{n,N,n',N'}(\omega) = \frac{4}{3}\sqrt{\frac{2\pi}{m_e T}}\,\frac{n_e e^4}{\hbar\omega}\,\Lambda^{\rm ff,\alpha}_{n,N;n',N'}(\beta_*, \omega/\omega_*), \tag{B4}$$

where for $\alpha = 0$

$$\Lambda^{\rm ff,0}_{n,N;n',N'}(\beta_*, \omega/\omega_*) = \frac{3}{2}\int_0^\infty \frac{{\rm d}u}{u'}\,{\rm e}^{-\beta_* u^2/2}\,\theta(u'^2) \times \sum_\pm (u' \pm u)^2\, w^{(0)}_{n,N;n',N'}(u_\pm), \tag{B5}$$

and for $\alpha = \pm 1$

$$\begin{aligned}\Lambda^{\rm ff,\alpha}_{n,N;n',N'}(\beta_*, \omega/\omega_*) &= \frac{3}{2}\int_0^\infty \frac{{\rm d}u}{u'}\,{\rm e}^{-\beta_* u^2/2}\,\theta(u'^2) \\ &\times \sum_\pm \left[\frac{m_*^2}{m_{\rm e}^2}\left(1-\alpha\frac{\omega_{\rm cp}}{\omega}\right)^2 w^{\rm e,\alpha}_{n,N;n',N'}(u_\pm) \right.\\ &+ \frac{2m_p m_e}{(m_{\rm p}+m_{\rm e})^2}\left(1-\alpha\frac{\omega_{\rm cp}}{\omega}\right)\left(1+\alpha\frac{\omega_{\rm ce}}{\omega}\right) w^{x,\alpha}_{n,N;n',N'}(u_\pm) \\ &\left.+ \frac{m_*^2}{m_{\rm p}^2}\left(1+\alpha\frac{\omega_{\rm ce}}{\omega}\right)^2 w^{\rm i,\alpha}_{n,N;n',N'}(u_\pm)\right].\end{aligned} \tag{B6}$$

Here $\beta_* = \hbar\omega_*/T = \hbar eB/m_* cT = \beta_p m_p/m_*$, and the arguments $u_\pm = [(u \pm u')^2 + u_{\rm s}^2]^{1/2}$, $u = |k_z| a_{\rm m}$, $u_{\rm s} = k_{\rm s}\, a_{\rm m}$, and

$$u' = \left[u^2 + \frac{2m_*}{m_p}(N - N') + \frac{2m_*}{m_e}(n - n') + \frac{2\omega}{\omega_*}\right]^{1/2} \tag{B7}$$

have the same meaning as in Appendix A. The functions $w(u_\pm)$ are defined as

$$w^{\rm e,+1}_{n,N;n',N'}(u) = \int_0^\infty \rho\,{\rm d}\rho\left[\sqrt{n'+1}\,\tilde v_{n,s,n'+1,s'-1}(\rho, u\sqrt2) - \sqrt{n}\,\tilde v_{n-1,s+1,n',s'}(\rho, u\sqrt2)\right]^2, \tag{B8a}$$

$$w^{\rm p,+1}_{n,N;n',N'}(u) = \int_0^\infty \rho\,{\rm d}\rho\left[\sqrt{N'}\,\tilde v_{n,s,n',s'-1}(\rho, u\sqrt2) - \sqrt{N+1}\,\tilde v_{n,s+1,n',s'}(\rho, u\sqrt2)\right]^2, \tag{B8b}$$

$$\begin{aligned}w^{x,+1}_{n,N;n',N'}(u) = \int_0^\infty \rho\,{\rm d}\rho &\left[\sqrt{n'+1}\,\tilde v_{n,s,n'+1,s'-1}(\rho, u\sqrt2) - \sqrt{n}\,\tilde v_{n,s+1,n',s'}(\rho, u\sqrt2)\right] \\ &\left[\sqrt{N'}\,\tilde v_{n,s,n',s'-1}(\rho, u\sqrt2) - \sqrt{N+1}\,\tilde v_{n,s+1,n',s'}(\rho, u\sqrt2)\right],\end{aligned} \tag{B8c}$$

where $s = N - n$ and $s' = N' - n'$ are the relative proton–electron orbital quantum numbers, and $\tilde v_{n,s,n',s'}(\rho, x)$ are the scaled Fourier transforms of the effective potentials defined in Appendix B of Potekhin & Chabrier (2003).[4] Due to the symmetry properties of these potentials we have $w^{({\rm e,p},x),-1}_{n,N;n',N'}(u) = w^{({\rm e,p},x),+1}_{N,n;N',n'}(u)$. Finally,

$$w^{(0)}_{n,N;n',N'}(u) = \int_0^\infty \rho\,{\rm d}\rho\,\tilde v^2_{n,s,n',s'}(\rho, u\sqrt2). \tag{B9}$$

One can demonstrate that the integrals (B8) are symmetric with respect to interchange of their indices n, n' or n, n', and moreover, all of them coincide with one another. It follows that equation (B6) simplifies to

$$\Lambda^{\rm ff,\pm1}_{n,N;n',N'}(\beta_*, \omega/\omega_*) = \frac{3}{2}\int_0^\infty \frac{{\rm d}u}{u'}\,{\rm e}^{-\beta_* u^2/2}\,\theta(u'^2) \times\left[w^{(1)}_{n,N;n',N'}(u_+) + w^{(1)}_{n,N;n',N'}(u_-)\right], \tag{B10}$$

where $w^{(1)}_{n,N;n',N'}(u)$ is any of the integrals (B8).

The integral (B10) diverges at $\omega \to \omega_{cp}(N' - N) + \omega_{ce}(n' - n)$, which is caused by the failure of Born approximation at slow electron–proton relative motion. As discussed in Section A1.4, this failure can be cured by introducing correction factors (A16) under the integral.

The functions $w^{(0,1)}_{n,N;n',N'}(u)$ can be presented as

$$w^{(\alpha)}_{nN;n'N'}(u) = \frac{1}{2}\int_0^\infty \frac{t^{|\alpha|}\,{\rm d}t}{(t + u^2/2)^2}\, I^2_{n',n}(t)\, I^2_{N'N}(t), \tag{B11}$$

This alternative representation can be obtained by passing from the cylindrical to Landau gauge in the derivation of the free–free cross-section (Appendix B of Potekhin & Chabrier 2003), taking into account equation (A3) and recurrence relation $L_n^s(x) - L_{n-1}^s(x) = L_n^{s-1}(x)$.

We see that $w^{(0)}_{n,N;n',N'}(u)$ coincides with $w_{n,N;n',N'}(u)$ given by equation (A19) at $Z_1 = Z_2 = 1$, Thus, for a given initial (n, N) and final (n', N') Landau quantum numbers, the effective rates of the electron–proton radiative and non-radiative transitions are determined, for any B, T, and ω, by one-dimensional integrals involving just two universal functions $w^{(0,1)}_{n,N;n',N'}(u)$. These functions are smooth and monotonically decreasing. At $u \ll 1$ they tend to constants, except for the following cases: (i) if $n' = n$ and $n' = n$, then $w^{(1)}_{n,N;n',N'}(u) \sim \ln u$ and $w^{(0)}_{n,N;n',N'}(u) \sim u^{-2}$; (ii) if $n' = n$ and $N' = N \pm 1$ (or $n' = n$ and $N' = N \pm 1$), then $w^{(0)}_{n,N;n',N'}(u) \sim n_* \ln u$, where $n_* = \max(N, N')$ (or $n_* = \max(N, N')$, respectively). At $u \gg 1$, $w^{(\alpha)}_{n,N;n',N'}(u) \propto u^{-4}$.

The approximation of infinitely massive ions (Pavlov & Panov 1976) is reproduced by setting $\omega_{\rm cp} = 0$ in equation (B1) and replacing $I^2_{N'N}(t)$ by $\sum_{N'=0}^\infty I^2_{N'N}(t) = 1$ in equation (B11).

Since equation (B1) is classical (although the factors $\nu_\alpha^{\rm ff}$ and $\tilde\nu_\alpha$ need quantum calculation), we may extend it to $Z > 1$. In this case the right-hand side of equation (B4) should be multiplied by Z^2, and the coefficient $\Lambda_{n,N;n',N'}$ will be different. By analogy with

[4] In equation (B7) of Potekhin & Chabrier (2003) the factor $\sqrt{\tilde s \tilde s'}$ (a typo) must be $\sqrt{\tilde s!\tilde s'!}$.

the general case of non-radiative Coulomb collisions, considered in Section A2.1, the latter difference consists in replacing of $I^2_{NN'}(t)$ by $I^2_{NN'}(t/Z)$ in equation (B11) and multiplying $(N - N')$ by Z in equation (B7). This simple generalization to the $Z \neq 1$ case is possible only in the adiabatic and Born approximations, which we use in this paper. Beyond these approximations, the effects of centre-of-mass motion of an ion–electron system affect the initial and final wave functions in a non-trivial way. Continuum wave functions with allowance for these effects have been so far calculated only for $Z = 1$ (Potekhin & Pavlov 1997).

This paper has been typeset from a TEX/LATEX file prepared by the author.